



Deliverable due date: (M12) M36 – (November 2017) November 2019

D4.8 Report on grid to vehicles strategies and performance
WP4, Task 4.3, Subtask 4.3.4

Transition of EU cities
towards a new concept of
Smart Life and Economy



Project Acronym	mySMARTLife		
Project Title	Transition of EU cities towards a new concept of Smart Life and Economy		
Project Duration	1 st December 2016 – 30 th November 2021 (60 Months)		
Deliverable	D4.8 Report on grid to vehicles strategies and performance		
Diss. Level	PU		
Status	Working		
	Verified by other WPs		
	Final version		
Due date	30/11/2019		
Work Package	WP4		
Lead beneficiary	VTT Technical Research Centre of Finland Ltd		
Contributing beneficiary(ies)	HEN		
Task description	<p>Task 4.3: Smart Energy Supply and Demand [HEN] (HEL, FVH, VTT, FOU, CAR)</p> <p>This task focuses on demonstrating technical integration of RES and storages in the district heating and cooling network with power production. The focus is in optimizing the production and reduction of system level CO₂ emissions. Important part of the optimization is the use of waste energy sources. The task also focuses on system level demand side management and optimization of the performance including reactive power control and balancing.</p> <p>- Subtask 4.3.4: G2V strategies - grid impact of the charging infrastructure</p> <p>VTT will demonstrate the technical integration of the EV charging point and the energy storage and the solar plant.</p>		
Date	Version	Author	Comment
03/05/2017	0.1	Anna Kulmala (VTT)	Structure of the deliverable and work planning
10/10/2017	0.2	Antti Alahäivälä (VTT)	EV charging background study and case Helsinki analysis. Suvilahti simulation.
27/11/2017	1.0	CARTIF	Alignment of contents and final review
7/5/2018	1.1	Antti Alahäivälä (VTT)	Study on EV charging load flexibility in Helsinki and its value with the Suvilahti BESS added.
28/2/2019	1.2	Kristiina Siilin (HEN)	Providing figures and contents to Chapter 9.1 (BESS demonstrations).
17/10/2019	1.3	Poria Divshali (VTT)	Add the simulation results of FCR flexibility in EV charging station of Helsinki area, adding Suvilahti field test results, and finalize the report

1/11/2019	1.4	Suvi Takala (HEN)	Reviewing the contents of Helen. Adding V2G performance test results to Chapter 9.
14/11/2019	1.5	Maria Viitanen Roope Husgafvel (HEL)	Internal review of deliverable
25/11/2019	2.0	Poria Divshali (VTT)	Final review

Copyright notices

©2017 mySMARTLife Consortium Partners. All rights reserved. mySMARTLife is a HORIZON 2020 Project supported by the European Commission under contract No.731297. For more information on the project, its partners and contributors, please see the mySMARTLife website (www.mysmartlife.eu). You are permitted to copy and distribute verbatim copies of this document, containing this copyright notice, but modifying this document is not allowed. All contents are reserved by default and may not be disclosed to third parties without the written consent of the mySMARTLife partners, except as mandated by the European Commission contract, for reviewing and dissemination purposes. All trademarks and other rights on third party products mentioned in this document are acknowledged and owned by the respective holders. The information contained in this document represents the views of mySMARTLife members as of the date they are published. The mySMARTLife consortium does not guarantee that any information contained herein is error-free, or up-to-date, nor makes warranties, express, implied, or statutory, by publishing this document.



Table of Content

1. Executive Summary.....	11
2. Introduction	13
2.1 Purpose and target group	13
2.2 Contributions of partners	13
2.3 Relation to other activities in the project.....	13
3. State of the Art—Smart Charging.....	14
3.1 Integration of EV charging to a power system	14
3.2 Electric vehicle charging environment	14
3.3 EV aggregator and its control strategies.....	18
3.4 Control of EV charging with local generation and storage.....	19
3.5 Pilot projects on the system integration of EVs	22
4. Power System Flexibility.....	23
4.1 Flexibility Market Regulations in Finland	24
4.2 EV Flexibility Model.....	24
5. Analysis of Electric Vehicle Charging in Helsinki	27
5.1 Data Pre-analysing	27
5.2 EV Behaviour	28
5.3 EV Growth.....	29
5.4 EV Flexibility	31
6. Suvilahti: System Description	32
7. Investigated Control Strategies for Suvilahti	35
7.1 Aim of the strategies	35
7.2 Exploiting the frequency control dead-band for the matching of local resources	35
7.3 Exploiting a part of the BESS's power capacity for the matching of local resources	37
7.4 Potential as a business case	39
8. BESS Simulation Studies on the Strategies.....	40
8.1 Aim of the simulations.....	40
8.2 Simulation setup and simulated cases	40
8.3 Results	44
8.3.1 Comparison of the control strategies	44
8.3.2 Sensitivity analysis.....	51
8.3.3 Result Summary	55
9. Demonstrations in Suvilahti.....	55

- 9.1 Demonstrations of Suvilahti BESS55
 - 9.1.1 Reserve power as a service for TSO.....56
 - 9.1.2 Peak shaving and time-shifting.....61
 - 9.1.3 Voltage support and reactive power compensation.....63
- 9.2 Performance tests with Suvilahti V2G charger65
 - 9.2.1 Test 1 - Up and down regulation in 5 kW steps at 10 seconds intervals.....66
 - 9.2.2 Test 2 – Up & down power regulation in 1 kW steps at 10 second intervals.....66
 - 9.2.3 Test 3 - composite run with different power regulation steps at 10 second intervals67
 - 9.2.4 Assumptions and possible sources or errors during the tests68
 - 9.2.5 Summary and conclusions of the tests with Suvilahti V2G.....69
- 10. Conclusions69
- 11. References.....71

Table of Figures

Figure 1: Different EV charging strategies for the system integration with their advantages and disadvantages as presented in (Garcia-Villalobos et al. 2014). 15

Figure 2: Illustration of different frameworks for EV charging. a) Home charging with one electricity supplier. b) Charging on private property, e.g., on an office building or a shopping mall. c) Charging in a public space. d) Home charging under the management of an EV aggregator. 17

Figure 3: EV aggregator’s service relationships in a smart grid environment. 19

Figure 4: Overview of aggregator’s control strategies according to (Hu et al. 2016). 20

Figure 5: Two stages of a smart charging algorithm and the required data inputs (Wi et al. 2013). 20

Figure 6: Illustration of a grid-connected EV charging station with PV generation and a storage element. 21

Figure 7: Energy Smart Home Lab at Karlsruhe Institute of Technology. 23

Figure 8: The charging profiles of EV: 1) Simple charging, 2) average power charging, 3) Providing some down-regulation flexibility. 25

Figure 9: The flexibility that an EV with a charging profile in Figure 5 can offer 26

Figure 10: a) The probability density of arrival time of EV to the charging stations during a day, b) The probability density for the number of charging start in the time interval (8:45-9) during the last year. 28

Figure 11: The probability density of EV charging duration and the best Weibull distribution fit to this probability density. 29

Figure 12: The probability density of EV charging energy (kWh) and the best Log-logistic distribution fit to this probability density 29

Figure 13: The monthly number of EV charging events 30

Figure 14: The average daily EV charging energy. 30

Figure 15: The cumulative density function (CDF) of FCR-N flexibility for different time of a day provided by EV. ... 31

Figure 16: The expected flexibility (FCR-N) provided by EV charged in Helsinki area. 32

Figure 17: Flexibility (FCR-N) growth during the last three years. 32

Figure 18: Helen Ltd’s energy storage in Suvilahti (Helen 2016) 33

Figure 19: V2G charging station in Suvilahti and its first charging (Picture: Helen Ltd) 33

Figure 20: Frequency control droop of the BESS in Suvilahti (Hellman et al. 2017). 34

Figure 21: Control strategy to provide FCR and to match local consumption and generation when the frequency is within the dead-band. 37

Figure 22: Control strategy to provide FCR and to match local generation and consumption with the offset power. SOC is targeted to be 50%. 38

Figure 23: Control strategy to provide FCR to match local generation and consumption with the offset power. 39

Figure 24: System frequency for an illustrative week in August 2016. 41

Figure 25: The generation of the Suvilahti solar power plant for one week in August 2016.41

Figure 26: EV charging load of 100 stations. The figure shows a randomly selected weekday and the expected charging profiles for a weekday and weekend day.....42

Figure 27: Measured SOC of the BESS (Hellman et al. 2017).44

Figure 28: Simulated SOC of the BESS. This is a snapshot from the simulation run over the two-month period (August and September 2016).....44

Figure 29: Illustration of Case 1 over a two-day period. In the uppermost subfigure, ESS indicates the offset power of the BESS. The net load is the sum of PV generation, EV charging, and the offset power. FCR is the activated reserve power by the BESS. Its SOC is depicted in the lowest figure.45

Figure 30: Illustration of Case 2 over a two-day period. In the uppermost subfigure, ESS indicates the offset power of the BESS. The net load is the sum of PV generation, EV charging, and the offset power. FCR is the activated reserve power by the BESS. Its SOC is depicted in the lowest figure.46

Figure 31: Illustration of Case 3 over a two-day period. In the uppermost subfigure, ESS indicates the offset power of the BESS. The net load is the sum of PV generation, EV charging, and the offset power. FCR is the activated reserve power by the BESS. Its SOC is depicted in the lowest figure.47

Figure 32: Illustration of Case 4 over a two-day period. In the uppermost subfigure, ESS indicates the offset power of the BESS. The net load is the sum of PV generation, EV charging, and the offset power. FCR is the activated reserve power by the BESS. Its SOC is depicted in the lowest figure.48

Figure 33: Illustration of Case 5 over a two-day period. In the uppermost subfigure, ESS indicates the offset power of the BESS. The net load is the sum of PV generation, EV charging, and the offset power. FCR is the activated reserve power by the BESS. Its SOC is depicted in the lowest figure.49

Figure 34: The exported and imported energies during the simulation period. The values contain only PV generation, EV charging, and the offset power of the BESS. That is, the energy needed for FCR is not included...50

Figure 35: The maximum export and import powers during the simulation period. The values contain only the sum of PV generation, EV charging, and the offset power of the BESS, i.e., the net load.....51

Figure 36: Percentage of time when the battery is nearly full or empty during the simulation. For example, 1% is approximately 14 hours (the studied period is two months).51

Figure 37: The sensitivities of the energy import and export on the import limits (x-axis in the subfigures) and export limits (different lines in the subfigures) with 20 EV charging stations. The limits are only used with cases 2, 3, and 5 so they are shown in the figure.52

Figure 38: Percentage of time when the battery is nearly full or empty and its sensitivity on the import limits (x-axis in the subfigures) and export limits (different lines in the subfigures). 20 EV charging stations.53

Figure 39: The sensitivities of the energy import and export on the import limits (x-axis in the subfigures) and export limits (different lines in the subfigures) with 100 EV charging stations. The limits are only used with cases 2, 3, and 5 so they are shown in the figure.....54

Figure 40: Percentage of time when the battery is nearly full or empty and its sensitivity on the import limits (x-axis in the subfigures) and export limits (different lines in the subfigures). 100 EV charging stations54

Figure 41: Target SOC was 50 % and the recovery power to target SOC during frequency dead band was 0 kW/200 kW.....57

Figure 42: Target SOC was 50 % and the recovery power to target SOC during frequency dead band was 0 kW/200 kW.....57

Figure 43: Target SOC was 50 % and the recovery power to target SOC during frequency dead band was 0 kW/200 kW.....57

Figure 44: Target SOC was 50 % and the recovery power to target SOC during frequency dead band was 200 kW.58

Figure 45: The SOC behaviour corresponding the regulation according to the curve in Figure 41 and recovery power to target SOC being 0 kW.....59

Figure 46: The SOC behaviour corresponding the regulation according to the curve in Figure 41 and recovery power to target SOC being 200 kW.....59

Figure 47: The SOC behaviour corresponding the regulation according to the curve in Figure 42 and recovery power to target SOC being 0 kW.....59

Figure 48: The SOC behaviour corresponding the regulation according to the curve in Figure 42 and recovery power to target SOC is 200 kW.....60

Figure 49: The SOC behaviour corresponding the regulation according to the curve in Figure 43 and recovery power to target SOC being 0 kW (until 2nd November)/200 kW.....60

Figure 50: The SOC behaviour corresponding the regulation according to the curve in Figure 44 and recovery power to target SOC is 200 kW.....60

Figure 51: Metro load causes varying power needs due to the acceleration and braking at the station.62

Figure 52: The battery (top) reacts to the metro peak power (middle) instantly and the reduced grid load is shown at the bottom.63

Figure 53: Reactive power compensation with the calendar-based schedule which takes into account the DSO needs.64

Figure 54: The BESS providing both voltage control and reactive power compensation depending on the time of the da65

Figure 55: The requested power profile and actual response of the charger during the test 1.....66

Figure 56: The requested power profile and actual response of the charger during test 2.....67

Figure 57: The requested power profile and actual response of the charger during test 3.....68

Table of Tables

Table 1: Contribution of partners	13
Table 2: Relation to other activities in the project.....	14
Table 3: The forecast of EV charging events' number and average daily energy in Helsinki area	31
Table 4: The availability for frequency regulation with different control parameters. 1C corresponds to a system where the power ratio to the energy is equal to one, e.g. in this case 600 kW / 600 kWh and 2 C corresponds to a system where power is double to the energy, e.g. in this case 1200 kW / 600 kWh.	61

Abbreviations and Acronyms

Acronym	Description
mySMARTLife	Transition of EU cities towards a new concept of Smart Life and Economy
BESS	Battery energy storage system
BEV	Battery electric vehicle
CP	Charging point
DSO	Distribution system operator
ESS	Energy storage system
EV	Electric vehicle
EVM	Electric vehicle meter
FCM	Final customer meter
FCR-D	Frequency containment reserve for disturbances
FCR-N	Frequency containment reserve for normal operation
PHEV	Plug-in electric vehicle
PV	Photovoltaic
SOC	State of charge
TSO	Transmission system operator
V2G	Vehicle to grid
VPP	Virtual power plant
FCM	the final customer meter
CP	: EV charging point

1. Executive Summary

The emergence of electric vehicles (EVs) in traffic shifts a part of the conventional transportation fuel usage to electricity demand. Consequently, the charging of EVs will not only ask for an additional generation in power system level, but it will also have an impact on the grid infrastructure. Particularly in the low voltage network, overloading is possible since the charging can increase peak demand. In order to assist the grid integration of EV, this deliverable investigates the control strategies for the charging.

The report firstly reviews the existing literature on EV charging. As EVs are becoming more common in the grid and their charging is a completely new type of load, their integration requires new infrastructure while it opens markets for new actors. Such actors are, for example, EV aggregators who provide services to EV owners and charging point managers who are able to provide charging services with their stations. In addition to the services provided to the EV owners, the aggregators can start to produce ancillary services to the grid and exploit the charging load flexibility when participating in the electricity markets. This naturally requires strategies for the control of the EV charging. The strategies can be classified into centralized, transactive and price-based control. The purpose of the control can vary but quite commonly EVs are seen as a potential resource for frequency control. The batteries of the EVs also provide energy storage to the grid, which can assist in the integration of renewable and variable energy sources, such as photovoltaic (PV), in the power system. One promising application is electric vehicle solar parking lots where PV generates the electricity for charging and EVs offer the storage for the generation.

Secondly, this report analyses the charging data recorded during the past years, from 2015 until 2018, from charging stations from the Helsinki area. The analysis revealed that half of the EVs' plug-in times are less than 98 minutes and that the charged energy is 10.4 kWh on average. The charging powers were not precisely known for the charging events but they were evaluated in order to get some understanding of the available flexibility. It was seen that half of the charging times are less than 53 minutes while half of the EV plugged for more than 98 minutes.

Thirdly, the co-operation of EV charging, battery energy storage system (BESS), and a solar power plant in Suvilahti was studied in the report. Different strategies were studied and compared in simulations. In the strategies, the BESS participated in the power system frequency control by continuously following the system frequency and adjusting its charging/discharging power. At the same time, it aimed to reduce electricity import and export, which were caused by the PV generation, EV charging, and the offset power of BESS. The ultimate goal of this approach is to improve the utilization of the local generation to supply local consumption. It was shown that the export and import power limits can be used to reduce energy import and export (better matching of local consumption and generation) but strict limits easily result in an

empty or fully charged battery. The control strategy of the BESS uses for frequency regulation also greatly affects the imported and exported energies.

Furthermore, this report presents field test results of the Suvilahti BESS and V2G charger. The results of frequency control, metro peak shaving, reactive power and voltage control tests done with the BESS are presented. In addition, three test runs with the V2G charger are discussed. The research phase of the Suvilahti BESS finished in summer 2019 and it will start operation in the TSO ancillary markets in the future and contribute to maintaining the power system frequency.

2. Introduction

2.1 Purpose and target group

This report examines the topic of electric vehicle grid integration as well as large battery storage control in grid-connected mode. Its main focus is on the control and charging strategies, which enable the integration in a coordinated manner. The purpose of the report is to create an overview of the existing charging approaches and develop new control strategies, which also consider the electric vehicle charging together with other distributed energy resources, namely battery energy storage systems and solar power generation. Furthermore, the report analyses the existing electric vehicle charging data available from Helsinki. The report is targeted to actors that are currently concerned about the grid integration of electric vehicle charging as well as to potential new actors, such as aggregators, who aim to create a business around the grid integration.

2.2 Contributions of partners

The following Table 1 depicts the main contributions from participant partners in the development of this deliverable.

Table 1: Contribution of partners

Participant short name	Contributions
VTT	The main responsibility of the deliverable
HEN	Contribution to chapters 4, 5, 6, 7 and writing contents of chapter 9.

2.3 Relation to other activities in the project

The following Table 2 depicts the main relationship of this deliverable to other activities (or deliverables) developed within the mySMARTLife project and that should be considered along with this document for further understanding of its contents.

Table 2: Relation to other activities in the project

Deliverable Number	Contributions
D4.1	Baseline report describes the starting situation of the actions
D4.6	Report on smart grid improvements
D4.7	Report on monitoring and control concepts and improvements
D4.17	Innovative electromobility charging node in operation

3. State of the Art—Smart Charging

3.1 Integration of EV charging to a power system

The number of passenger cars charged from the electric grid is expected to grow considerably in the near future (Eurelectric 2015). The emergence of these battery electric vehicles (BEVs) and plug-in electric vehicles (PHEVs) in traffic shifts a part of the conventional transportation fuel usage to electricity demand. In power system level, this will ask for an additional generation but the effects of charging are likely to be visible also in the low voltage network, where the charging is expected to occur (Eurelectric 2015). So-called dummy charging can increase peak demand: once people arrive home, they start charging electric vehicles (EVs) as a result of which the charging coincide with the already existing evening peak consumption. Power peaks can cause overloading or voltage drops and may eventually increase the cost of electricity infrastructure. Therefore, the integration of EVs in the power system and distribution grid should be given attention.

As stated in (Garcia-Villalobos et al. 2014), an electric vehicle can be a simple electrical load, a flexible electrical load, or a distributed and mobile storage element, depending on the integration of EV charging and the utilized control strategies. Some charging integration strategies with their advantages and disadvantages are illustrated in Figure 1. The peak shaving smart charging strategy presented in the figure assumes vehicle-to-grid (V2G) ability, i.e., EV battery can be discharged to the grid. In addition to these approaches, the EVs can be employed to provide different ancillary services to the grid, such as frequency and voltage control.

3.2 Electric vehicle charging environment

The literature covers a considerable amount of research focusing on the system integration of EVs. Here, of particular interest are different charging strategies, enabling the manipulation of the charging load. Each strategy requires certain interaction between existing and potential new agents in the electric system and

markets. The conventional agents are distribution system operator (DSO), transmission system operator (TSO), electricity supplier or retailer, and the final customer, whereas according to (San Roman et al. 2011), potential new agents are:

- EV owner: an agent that owns an EV and requires electricity to charge it. The reader should note that an EV owner is not necessarily the same as the conventional final customer.
- EV aggregator: aggregator is an entity who can utilize EVs to provide flexibility and ancillary services to the power system and in the same time they may be a supplier (retailer) who sells electricity to EV owners
- EV charging point manager: agent that has the charging infrastructure on private property and that buys and resells electricity for the charging on its property. The charging point manager can be, for example, a residential customer, an office building owner, a commercial building owner, or a charging station owner.

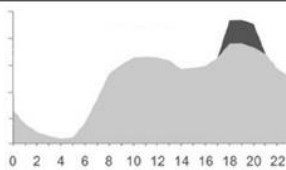
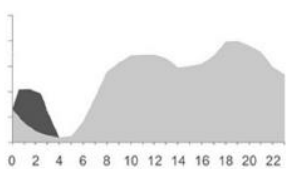
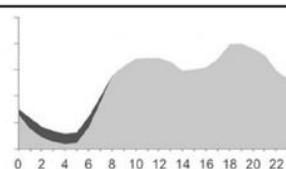
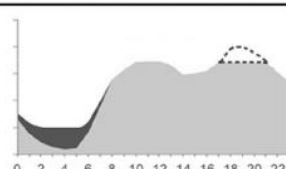
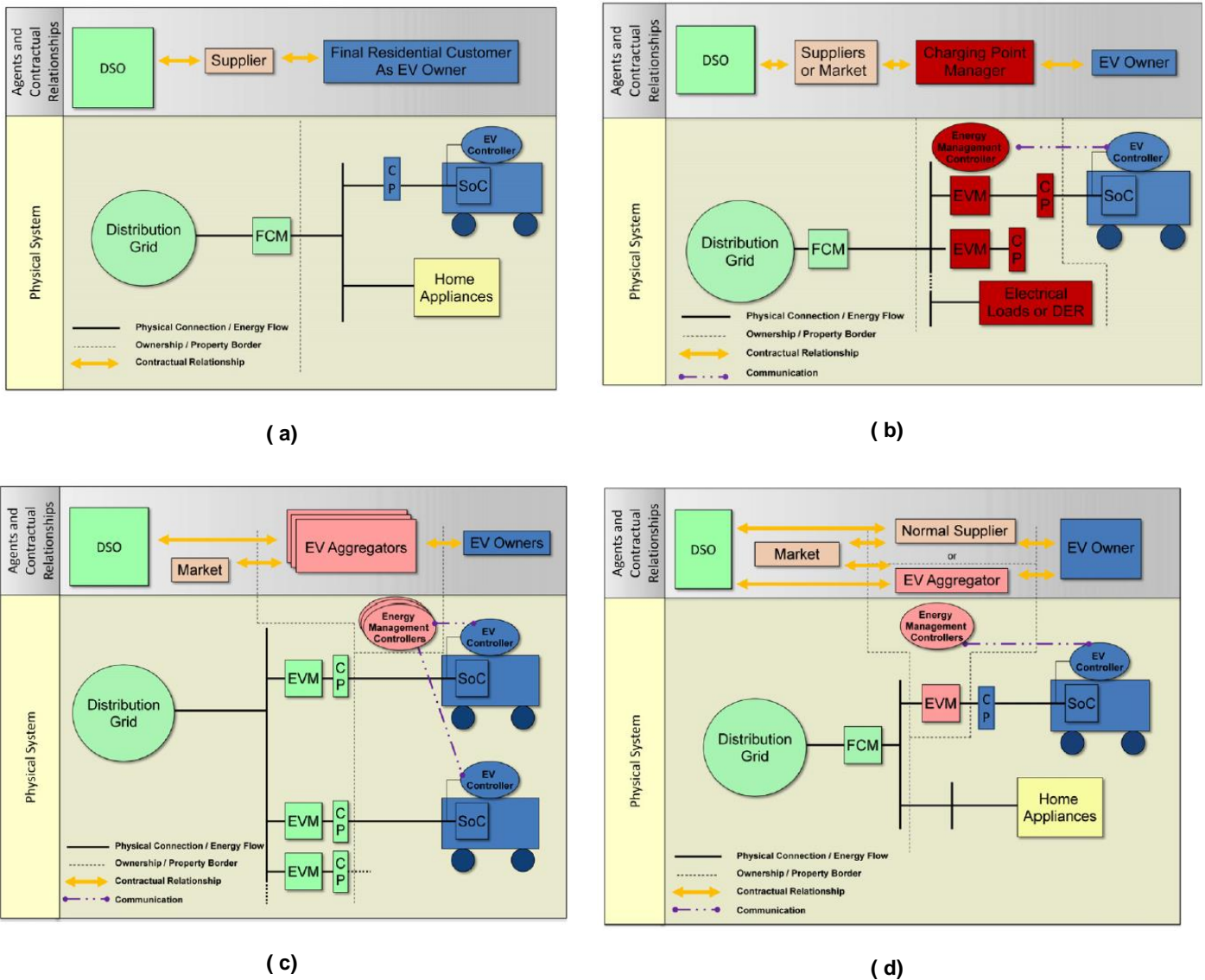
		Advantages	Drawbacks
Uncontrolled Charging		<ul style="list-style-type: none"> ✓ Easy implementation ✓ User friendly 	<ul style="list-style-type: none"> × Overload of transformers and lines × Voltage deviations × Peak power increase × Increase of electricity CO₂ intensity × Electricity cost increase × Needs to reinforce the grid
Off-peak Charging		<ul style="list-style-type: none"> ✓ Easy implementation ✓ Demand profile flattened ✓ Better integration of wind energy at off-peak hours ✓ Delay in grid investments 	<ul style="list-style-type: none"> × Imbalances due to rapid increase of power consumed by PEVs × Possible overload of transformers and lines × Possible voltage deviations × Willingness of the customer required
Smart Charging (Valley filling)		<ul style="list-style-type: none"> ✓ Ancillary services provision ✓ Demand profile flattened ✓ Better integration of wind energy at off-peak hours ✓ Delay in grid investments 	<ul style="list-style-type: none"> × Complex implementation × ICT technologies required × Willingness of the customer required
Smart Charging (Peak saving)		<ul style="list-style-type: none"> ✓ Ancillary services provision ✓ Peak power reduction ✓ Optimal integration of intermittent RES ✓ Reduction of electricity CO₂ intensity ✓ Less investments in network reinforcements 	<ul style="list-style-type: none"> × Very complex implementation × ICT technologies required × Willingness of the customer required × Premature degradation of batteries resulting of using V2G × Energy losses in grid-battery-grid transmissions

Figure 1: Different EV charging strategies for the system integration with their advantages and disadvantages as presented in (Garcia-Villalobos et al. 2014).

The authors in (San Roman et al. 2011) also visualize different charging options illustrating the interaction between the agents. The base case is provided in Figure 2a, where the EV owner is also a final customer

and the charging is done at home. Electricity for the charging is supplied by the same agent (retailer) that also sells the electricity to the household. Next, charging in an office building with its own management system is presented in Figure 2b. The EV owner can be, for example, an employee in the office and the charging point manager the owner of the building. The charging point manager sells the electricity for the charging, as well as manages it in order to maximize own profit or minimize payments paid to the electricity supplier. Figure 2c showcases public street parking with multiple potential EV suppliers. This case assumes that the local DSO provides the charging infrastructure for public charging. The infrastructure is available for different EV aggregators who can establish their business and compete with each other once they pay regulated fees to the DSO. The EV owners, instead, make contracts with aggregators that best suit their needs. Lastly, home charging with an EV aggregator is illustrated in Figure 2d. The household can basically have two suppliers: the EV aggregator who supplies and manages the EV charging and a conventional retailer, providing the electricity for the rest of the loads. Separate meters need to be installed for the EV and the household consumption so that the two suppliers can settle their contracts based on the measurements.



The colours indicate assets that are owned and operated by a particular agent, e.g., green indicates the assets owned and operated by the DSO.

Figure 2: Illustration of different frameworks for EV charging. a) Home charging with one electricity supplier. b) Charging on private property, e.g., on an office building or a shopping mall. c) Charging in a public space. d) Home charging under the management of an EV aggregator.

In Figure 2, the charging infrastructure is owned by either a final customer, a charging point manager or a DSO. As stated in (Madina et al. 2016), there can also be a separate charging service operator who is responsible for the charging infrastructure. The operator manages the charging process as well as monitors, maintains, and controls its charging stations. Furthermore, it offers services to electro-mobility service providers as, for example, to the EV aggregators who further contract with end-users. What comes

to the charging related data, the charging service operator owns all data related to charging stations and the aggregator is the owner of EV user data.

3.3 EV aggregator and its control strategies

Generally, the requirement for a certain entity, providing charging services to EV owners, has been widely accepted. It can be referred to as an EV aggregator, an electro-mobility service provider, or an EV fleet operator. The aggregator's, or fleet operator's service relationships in a smart grid are illustrated in Figure 3 (Hu et al. 2016). As proposed by the figure, the aggregator's main goals are:

- Management of the charging in such a way that the EV owners' charging needs are satisfied and that the cost of the charging is minimized.
- Provide ancillary services (congestion prevention, voltage regulation) to DSO
- Provide ancillary services (up/down regulation, spinning reserves) to TSO
- Provide storage services to renewable energy source supplier.

Since the aggregator is likely to operate in a market environment with several competitors, its objective is also to remain profitable. That is, it should provide attractive services and prices to the EV owners in order to get customers while keeping costs low. The costs consist of potential control and ICT infrastructure investments, or the payment due to its usage, and the procurement of electricity for the charging from markets. Income the aggregator can get from electricity and ancillary service selling and the selling of other mobility-related services.

In order to achieve its goals, the aggregator needs to apply different control strategies, which schedule and control the EV charging. In (Hu et al. 2016), the control strategies are divided into three: centralized, transactive, and price control and they are shortly summarized and compared in Figure 4. As implied by the name of the strategy, the centralized control is based on central decisions made by the aggregator. The aggregator can receive status information from EVs, such as their current state of charge (SOC), and it can send direct control signals (e.g., charge/discharge, charging power) to the cars. Potential goals for the control is to minimize the EV charging cost or to maximize the profit of providing regulation services (ancillary services). In the case of the transactive strategy, the aggregator and EVs go through a negotiation process, which aims to produce an agreement between them. For example, the aggregator updates the sent price as long as equilibrium, and good enough load profile is achieved. Price control, instead, does not need the iteration: the aggregator communicates a price signal to EVs, which decide their response locally, i.e., they can simply do nothing or they can aim to minimize their charging cost. Nevertheless, the aggregator needs to predict the price elasticity of the EVs.



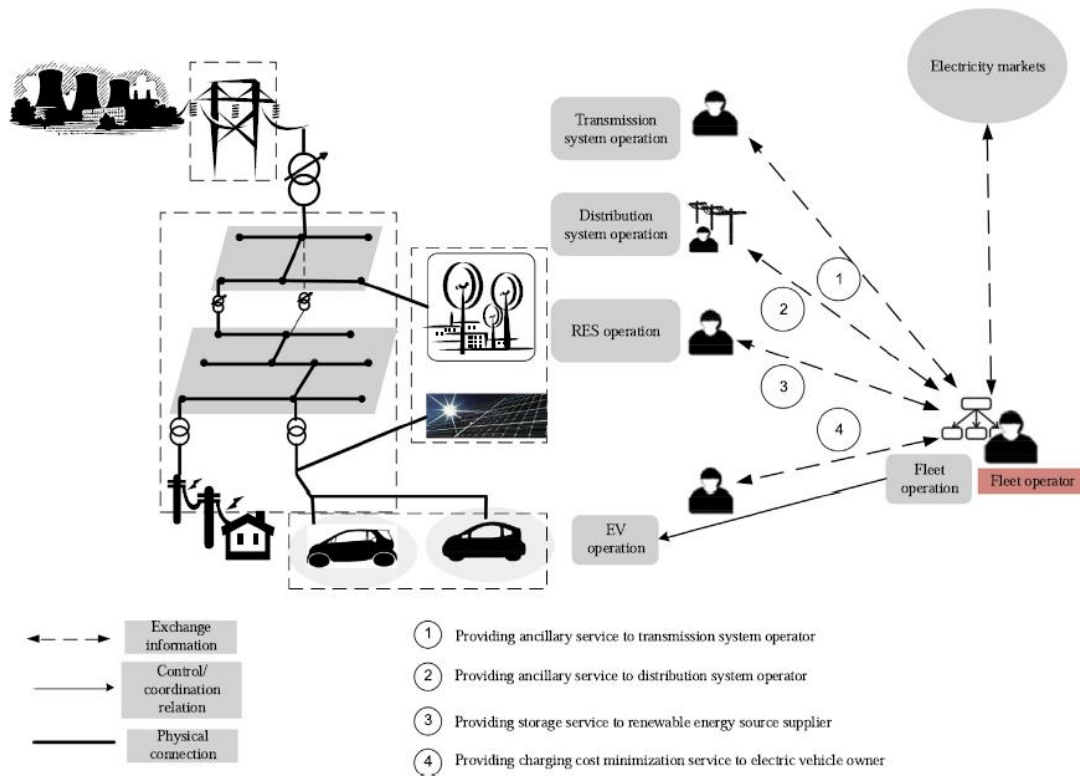


Figure 3: EV aggregator's service relationships in a smart grid environment.

3.4 Control of EV charging with local generation and storage

With the price control, an aggregator basically aims to produce a favourable load profile for its own purposes, e.g., reduce peak load or shift the consumption to hours when the procurement price of electricity from markets is low. On the other hand, the customers aim to minimize their electricity cost by employing their local resources in such a way that high electricity price periods are avoided. In addition to EVs, price control can be applied to households, offices, or other end-users in general. The end-users can have local energy storages, generation, flexible loads, and EVs, which they utilize optimally. One example of such an approach is proposed in (Wi et al. 2013) where EV charging scheduling algorithm is used to minimize the electricity cost of a building with PV generation. Their approach consists of the two stages illustrated in Figure 5. Firstly, PV generation and the electricity consumption of the building are forecasted. Secondly, the forecasts are updated based on the weather and optimization model is initialized and solved. The optimization allocates the EV charging so that the cost of electricity import from the grid is minimized and the target SOC set by the user is achieved at the moment of departure.

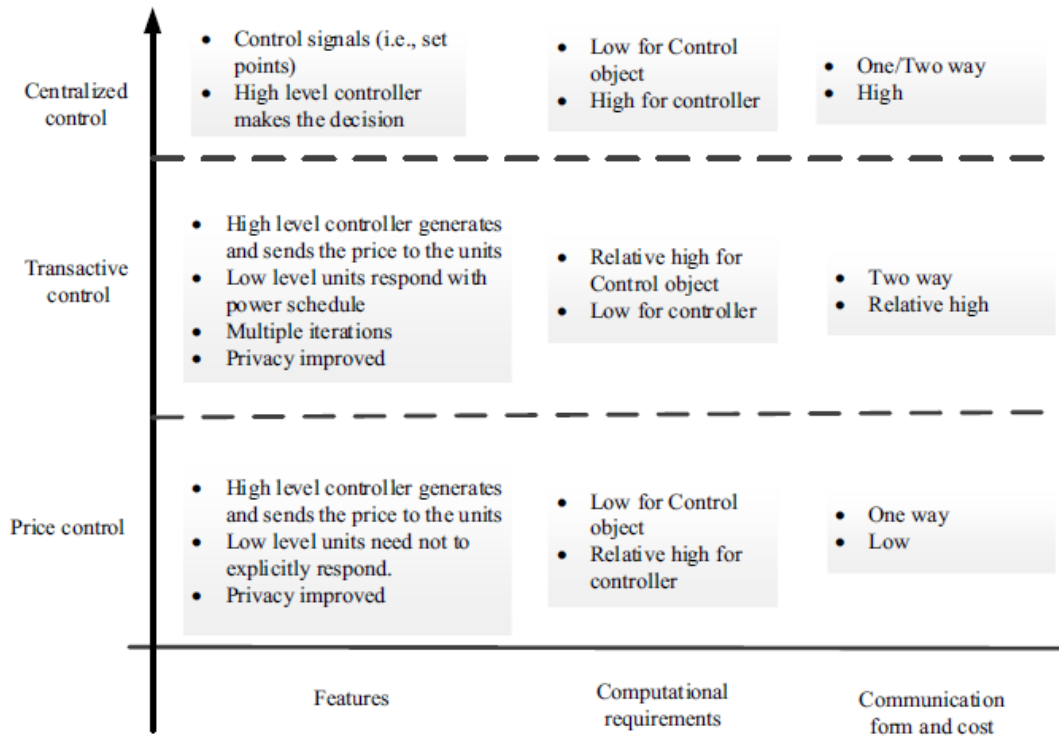


Figure 4: Overview of aggregator’s control strategies according to (Hu et al. 2016).

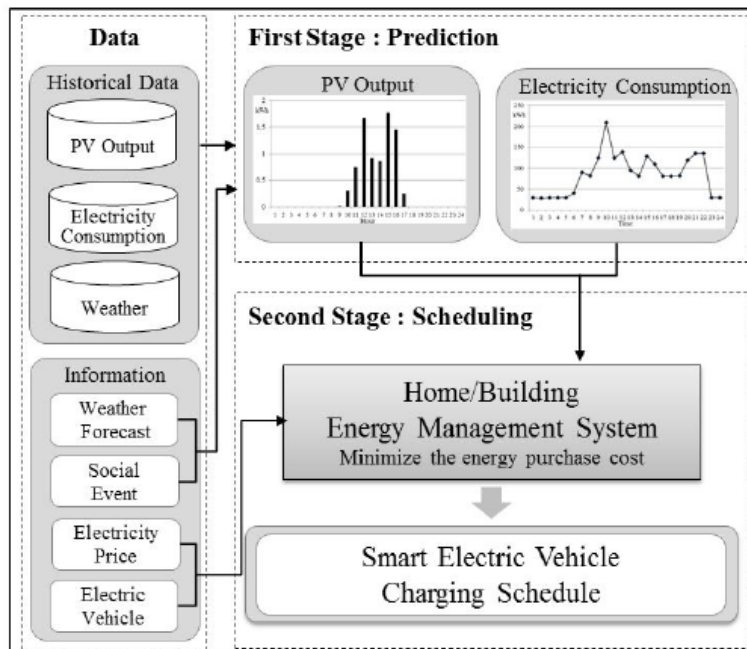


Figure 5: Two stages of a smart charging algorithm and the required data inputs (Wi et al. 2013).

Another promising approach to combine EV charging and PV generation is electric vehicle solar parking lots (Nunes et al. 2016). The motivation for these parking lots arises from the system integration challenges of EV and PV, which could be mitigated with the parking lots: the intermittency of PV generation can be reduced by employing the storage capacity of EVs while the charging load demand becomes supplied. The electric vehicle solar parking lots may be public or private and they are applicable nearly everywhere, including private housing, workplaces, shopping malls and transportation-related parking (e.g. train stations and airports). The authors of (Nunes et al. 2016) write that the benefits of the parking lots are the charging of EVs with clean energy, the provision of sunshade and protection for vehicles, no competition for land, and the possibility of the parking place to act as an EV aggregator. However, electric vehicle solar parking lots require a considerable amount of control in order to obtain a high utilization of PV generation. Further, the variability of the generation and the stochastic nature of the EV parking and electricity demand increase the complexity of the system. Ability to V2G would be advantageous but it reduces battery lifetime. The authors also state that more field-testing is required, whereas theoretical knowledge already exists. Lastly, the drivers' willingness to pay and their demand for the service are still open questions.

One example of a grid-connected EV-PV charging station is depicted in Figure 6, originating from (Bhatti et al. 2016). The system also comprises a separate energy storage system, which can store excess PV generation and mitigate grid loading when charging is done with high power (or the demand is otherwise high). As seen in the figure, the system can be implemented with a common dc bus, i.e., PV, storage, and EVs are connected to direct current system via their power electronic interface. The dc bus is further connected to the main grid with an inverter. Such an approach can reduce conversion losses and thus, improve the efficiency of the charging station.

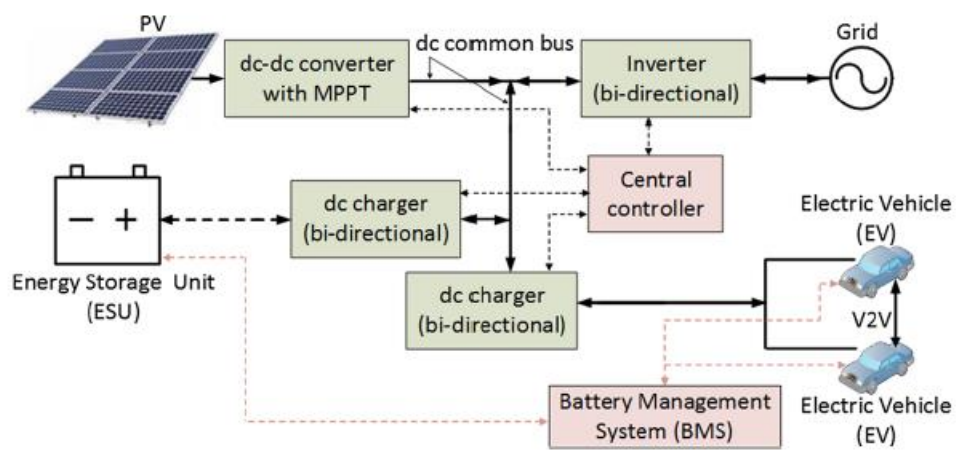


Figure 6: Illustration of a grid-connected EV charging station with PV generation and a storage element.

Lastly, virtual power plants (VPPs) and electricity retailers and aggregators can also assist in the integration of EV charging to the electrical system with distributed generation and other controllable resources. VPPs are an option to aggregate distributed resources so that they can collaboratively act as a single unit in a power system. This increases the visibility and controllability of resources, as a result of which they fit better to the current power system structure and the electricity markets. VPPs can be classified into commercial and technical plants (Pudjianto et al. 2007). The former participates in the markets where it optimizes its revenue, whereas the latter concentrates on the management of the local electricity grid.

Electricity retailers also benefit from the flexibility provided by the distributed energy resources, such as EVs. For example, in (Ghazvini et al. 2015), the retailer utilizes the flexibility to hedge its financial risk in a wholesale electricity market (day-ahead market). Due to the uncertainty associated with day-ahead decisions, a possibility to adjust the consumption may be advantageous. Thus, the retailer provides monetary incentives to price-elastic loads in order to motivate load reduction during certain hours.

3.5 Pilot projects on the system integration of EVs

The smart charging of EVs has been already investigated in several pilot projects. The following lists some recent projects piloted charging strategies, and observations:

- **Smart Solar Charging:** a demo project which aimed to develop control algorithms to utilize EV battery to improve the own use of solar power in the residential sector. In their case study, the developed control strategies increased the self-consumption of PV with 23% to 38%, while power peaks were reduced with 27% to 67% (Smart Solar 2017).
- **BMW i ChargeForward:** 96 EVs and battery storage were aggregated so that they provided a load reduction capacity of 100 kW to the system's TSO (CAISO). If the TSO requests for load reduction, the charging is delayed and the battery storage is used to provide the rest of the requested capacity if EVs cannot provide sufficient reduction. The battery storage was a part of a microgrid system, comprising also an office building and local PV generation (BMW i ChargeForward 2017).
- **Smart Charging & the ChargeTO Pilot:** so-called paired smart-charging was piloted. The charging strategy was employed for load shifting so that the users set the time they need the battery to be fully charged. The load was controlled by the utility (Stevens 2016).
- **EVGI Research Overview at NREL:** EV charge management with renewable sources was piloted. The charging stations located in a parking garage take input data (e.g. departure time) from users. This data from the stations are further aggregated. A central controller employs the aggregated data, energy price, facility load, and renewable energy production and optimizes the charging (Kisacikoglu 2016).

- **SEEV4-City:** The main objective of the project is to demonstrate smart electric mobility solutions, integrating renewable energy production, and to encourage their take-up in cities. The project pilots the interaction of EVs and renewable energies in different situations, including vehicle2home, vehicle2business, and vehicle2neighbourhood (SEEV4-City 2017).
- **Intelligent Zero Emission Urban System–iZEUS:** in the project, vehicle to grid based on the new ISO/IEC 15118 standard was demonstrated in Energy Smart Home Lab that is shown in Figure 7 (iZEUS 2014).

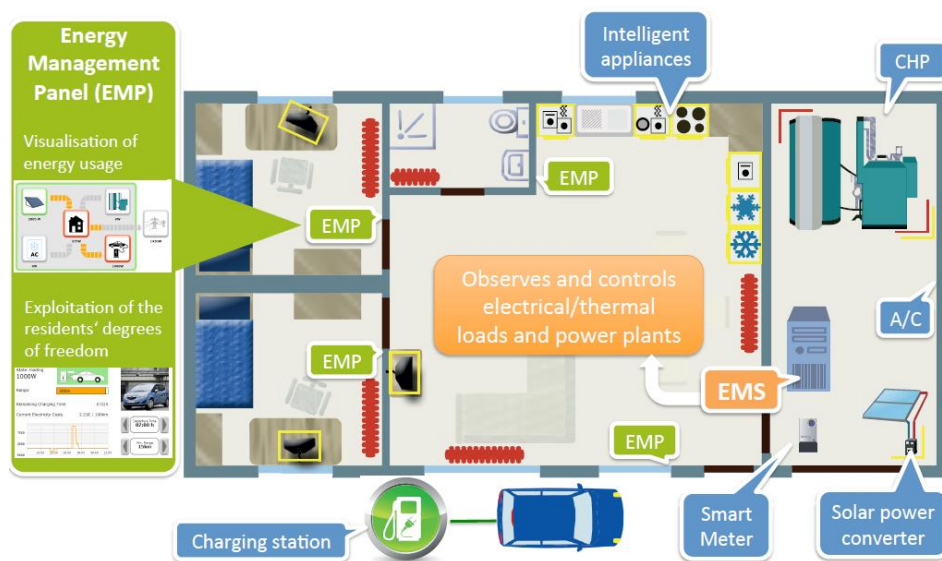


Figure 7: Energy Smart Home Lab at Karlsruhe Institute of Technology.

4. Power System Flexibility

Power system flexibility is generally defined as the ability of the power system to adapt to dynamic and changing conditions, e.g. changes in load and generations, in periods of minutes to over years (EPRI). This general definition of power system flexibility is not comprehensive and cannot be used for quantitative analysis of the EV potential in providing flexibility. Therefore, in order to analyse EV flexibility, this section proposes a concrete definition of flexibility based on operating flexibility markets. Since the available EV data is for the Helsinki area, this paper focuses on the Finnish flexibility market. However, almost similar market regulations are available in other countries, especially in Europe, as explained in more details in the deliverables of RealValue (Nolan Ritter, etc 2017) and SmartNet (Julia Merino , Inés Gómez , Elena Turienzo, 2016) projects.

4.1 Flexibility Market Regulations in Finland

The Finnish electricity market has one of the most conducive frameworks among European countries for flexibility of loads and generations. At the moment, demand flexibility can participate in eight different market places (Nolan Ritter, etc 2017). Investigating all of these markets is beyond the scope of this deliverable. Here, the frequency containment reserve for normal operation (FCR-N), which has the highest reimbursement level, is analysed.

The aim of FCR-N is to keep the power system frequency near the nominal value during normal dynamic disturbances. The Nordic transmission system operators (TSO) divide the obligation of FCR-N between subsystems proportional to annual energies used and the share of Finland is about 140 MW (FINGRID). In 2018, the price for yearly contracted capacity in Finland was 14 €/MWh while the energy provided is remunerated according to the up-regulating market price. A daily market is available for all flexibility providers. The yearly contracted resources are obliged to bid their promised amounts on the daily market. The minimum amount for participation is 100 kW.

FCR-N providers are expected to activate the reserves symmetrically in both directions (up- or down-regulation) within 5 to 20 seconds when the frequency deviates from the nominal value. The flexibility resources must provide their service as long as the frequency is out of the nominal range and they can come back to their nominal consumption/ production when the grid frequency is more than 49.9 Hz for at least three minutes. However, for reserve units with limited capacity, e.g. storage systems, the regulation requires the ability to continue full activation at least for 30 minutes.

4.2 EV Flexibility Model

The flexibility of an EV charging comes from the fact that most of the time an EV is connected to the grid longer than is required for charging. Figure 5 shows a charging profile of an EV connected to the grid at t_a and departure at t_d , with a need for E kWh of electrical energy. The minimum time (t_{ch}) for charging E kWh energy of the EV can be calculated by:

$$t_{ch} = \frac{E}{P_{max} \eta} \quad (1)$$

where P_{max} is the maximum power of EV chargers and η is the efficiency of the charger. If $(t_d - t_a)$ is longer than t_{ch} , the EV has some flexibility to alter its charging power curve to adapt itself to the power system dynamics without making any change in the energy-charged in the battery at the end of the period. In order to model this flexibility based on FCR-N definition, it is important to consider the following requirements:

Average Power: Since the main aim of connecting an EV to the grid is to charge the battery, providing flexibility should not change the amount of the charging energy. It means the average charging power (P_0)

of EV in any charging profile must be kept equal to $P_0 = E/(t_d - t_a)$. In other words, if the EV increase the charging power by F kW above the average for providing down-regulation flexibility during a period (t_f), it will need to decrease the average power after the flexibility period to keep the average the same (if the battery size does not allow extra charging), and vice versa.

Figure 8 shows the EV charging profile with the average power (P_0) and one alternative down-regulation flexibility (F kW) for t_f hours. It is important to notice that down-regulation is defined as a decrease in generation or increase in demand and in the same way up-regulation can be defined.

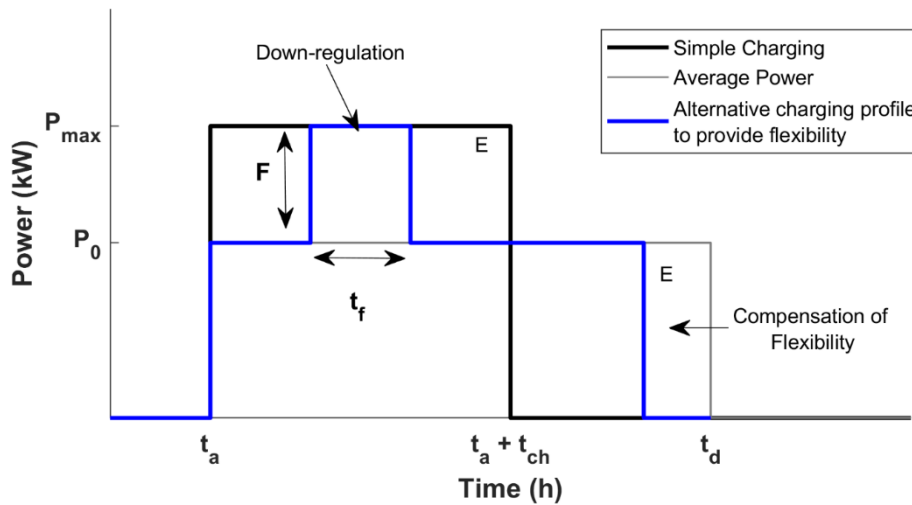


Figure 8: The charging profiles of EV: 1) Simple charging, 2) average power charging, 3) Providing some down-regulation flexibility.

Duration: In FCR-N, the duration of the activation (t_f) depends on the network situation. However, as mentioned in the market regulations, the worst-case scenario is 30 minutes. Since the flexibility provided by EV needs to compensate in the opposite direction to keep the charged energy fixed at E kWh (see Figure 5), an EV may not be able to offer a fixed amount of flexibility during the charging period. The maximum flexibility that EV can offer in time t in down-regulation (F_{down}) can be calculated by:

$$F_{down}(t) = \max\left(0, (P_{max} - P_0) * \min\left(1, \frac{P_0 * (t_d - (t + 0.5))}{(P_{max} - P_0) * 0.5}\right)\right) \tag{2}$$

where P_0 is the average power and $(P_{max} - P_0)$ is the maximum power increase that each EV can provide at time t when they are charging by the average power (see Figure 5). The term $\min(1, \dots)$ in (2) guarantees to have enough time to compensate the power increase for half an hour (the worst-case scenario) in the remaining time $(t_d - (t + 0.5))$ in order to keep the total energy fixed. The term $\max(0, \dots)$ removes all negative values.

In the same way, the maximum flexibility that EV can offer in time t in up-regulation (F_{up}) can be calculated by:

$$F_{up}(t) = \max\left(0, P_0 * \min\left(1, \frac{(P_{max}-P_0)*(t_d-(t+0.5))}{P_0 * 0.5}\right)\right) \tag{3}$$

where P_0 is the maximum power decrease that each EV can provide (regardless vehicle to grid); and the second term of the equation ($\min(1, \dots)$) guarantees that there is enough time to compensate this decrease in charging power of EV to keep the total energy fixed.

It is important to notice that if the battery size allows, it is possible to charge the EV more than E ; in other words, down-regulation could be provided without paying attention to the second term of (3). However, since the data of the initial charge of EV and the battery size are not clear for charging stations at the moment, this paper selects a conservative approach and keeps the EV energy the same when offering the flexibility.

Symmetrical Direction: According to the market regulations, reserve in FCR-N should have the ability of activation symmetrically in both up-regulation and down-regulation. Therefore, the amount of flexibility (F), which can be provided by an EV, will be

$$F(t) = \min(F_{up}(t), F_{down}(t)) \tag{4}$$

Using the above-mentioned requirements, Figure 9 depicts the flexibility that an EV, with a charging profile shown in Figure 8, can offer. In the same way, a group of EV can offer flexibility that can be formed by the aggregating each individual flexibility.

It is important to notice that the connecting time, departure time, and charging energy of EV are random variables. In the next section, the probabilistic distributions of these random variables are obtained using real data measurements of the Helsinki area. Then, the EV flexibility will be formed based on these probabilistic distributions.

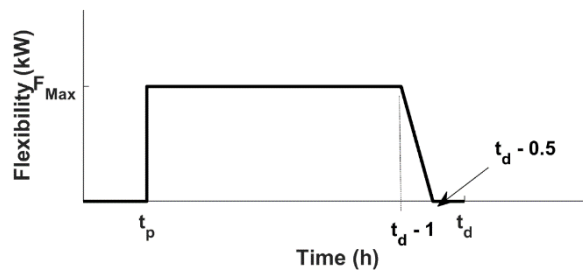


Figure 9: The flexibility that an EV with a charging profile in Figure 5 can offer

5. Analysis of Electric Vehicle Charging in Helsinki

This section investigates the potential of empirical EV behaviours in providing the FCR-N flexibility by analysing the charging records of EV charging stations in the Helsinki area. The charging stations do not have access to EV information, such as EV type, the battery size, and the charger size. They just record all charging events, which includes:

- The customer ID encrypted due to data protection rules,
- The station ID, and the maximum station power,
- The arrival and departure time,
- The charged energy (kWh).

Since the recording data includes several meaningless records, it is necessary to clean-up and pre-analyse the data before using for the flexibility model.

5.1 Data Pre-analysing

The data used in this project includes about 53,000 charging events of EV charging stations at the Helsinki area from Oct 2014 until Oct 2018. Some of these data include missing items or meaningless information. Therefore in clean-up, all events presenting one of the following issues:

- Missing items,
- Duration plug-in less than five minutes
- Energy charged less than 0.1 kWh or more than 100 kWh
- Charging power more than the charging station rate

are removed, which includes about 32% of the data.

The charging power of each EV is not in the event data, but in this research, the maximum charging power of the i th EV ($P_{max,EV,i}$) is estimated by the maximum average power among all charging events of i th EV ($P_{av,Event,i}$) while using onboard charger as follows:

$$P_{max,EV,i} = \max(P_{av,Event,i} | P_{av,Event,i} < 30), \quad (5)$$

where $P_{av,Event,i}$ can be calculated using the charged energy, arrival and departure time of the EV. It is important to notice that if the EV uses the AC power, the charging power is limited by the size of the onboard charger. However, if they use the DC power, the onboard charger is bypassed and the charging power is limited by the DC charger size of the charging station. In the Helsinki area, most of the EV

charging stations provide AC charging with a power rating of less than 30 kW, while some others provide DC charging with higher power rate.

5.2 EV Behaviour

After the cleaning process, the EV charging records include about 2450 customer IDs and 35500 charging events. It means almost 14 charging events on average per customer in three years. This data are not enough for precise prediction of EV behaviour. This subsection analyses the probability distribution of EV behaviour and the next subsection analyses the EV growth.

Figure 10.a shows the probability density of the EV arrival time to the charging stations during a day. This probability density can be used to allocate the number of charging events per day to different time intervals. For instance, the probability related to the time interval (8:45-9) is 0.03 which means in a day with 33 charging events, it is expected one event to start at this time interval. However, it is the expected value and the real value in each day could be different. Figure 10.b shows the probability density for the number of charging started in the time interval (8:45-9) during the last year.

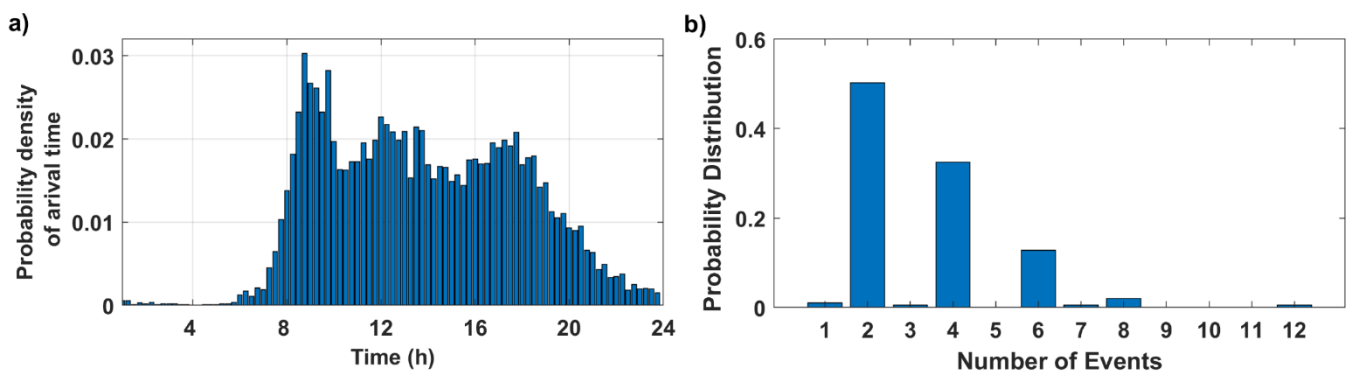


Figure 10: a) The probability density of arrival time of EV to the charging stations during a day, b) The probability density for the number of charging start in the time interval (8:45-9) during the last year.

Figure 11 shows the probability density of EV charging duration. The average EV charging time in the Helsinki area is 2 hours and 48 minutes. However, the longest one is more than 14 days. The best probability density function, which can represent the EV charging duration is the Weibull distribution having shape and scale parameters equal to 2.620 and 0.898, respectively.

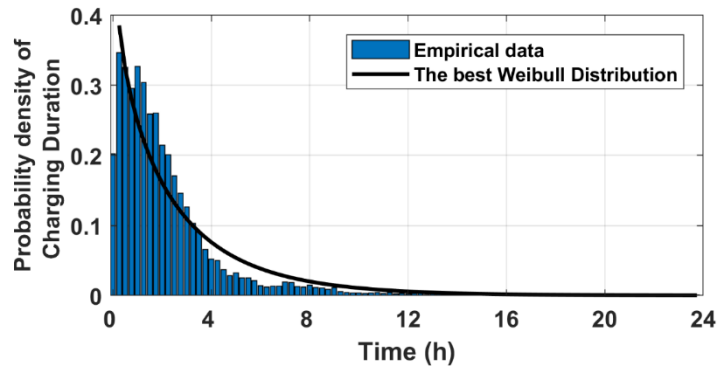


Figure 11: The probability density of EV charging duration and the best Weibull distribution fit to this probability density

Figure 12 shows the probability density of EV charging energy (kWh). The average charged energy of an EV in a charging event is about 10 kWh. The best probability density function, which can represent the EV charging energy, is the Log-logistic distribution having shape and scale parameters equal to 1.827 and 0.566, respectively.

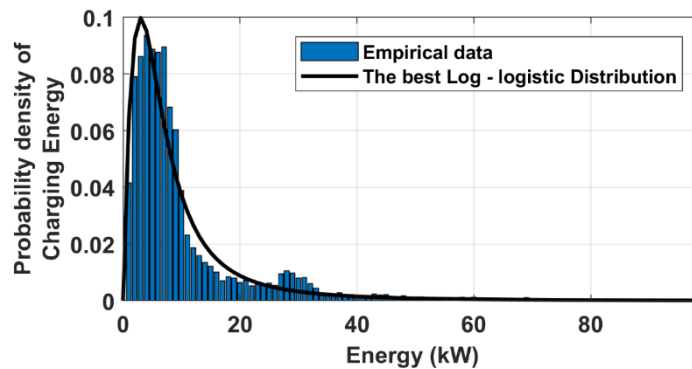


Figure 12: The probability density of EV charging energy (kWh) and the best Log-logistic distribution fit to this probability density

The probability distribution function of EV charging accompanies with the expected charging energy can give a comprehensive understanding of the future threat and potential of EV on power systems. For this reason, in the next subsection, the charging event and energy growth of EV in the Helsinki area are analysed.

5.3 EV Growth

The number of charging events and the average daily charging energy of EV are practical indicators of EV growth. In this regards, Figure 13 demonstrates the number of charging events per month in Helsinki area from 2015 until 2018, which shows a rapid growth with some fluctuation. This fluctuation in the number of

EV charging is resulted due to the natural behaviour of EV drivers, e.g. summer vacation time, and could also be caused by the clean-up process of data (see Section III. A).

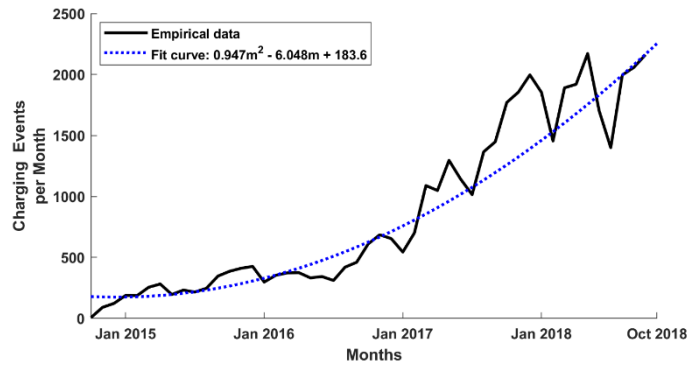


Figure 13: The monthly number of EV charging events

Figure 14 shows the average daily charging energy of EV per month. The energy consumption of EV almost has the same growth as the number of charging events in Figure 13. It shows that although the number of EV and EV charging stations have increased during this period, the average energy per event has not changed that much. This fixed average energy per event accompanied by faster chargers in the future will result in a higher potential for EV to provide flexibility.

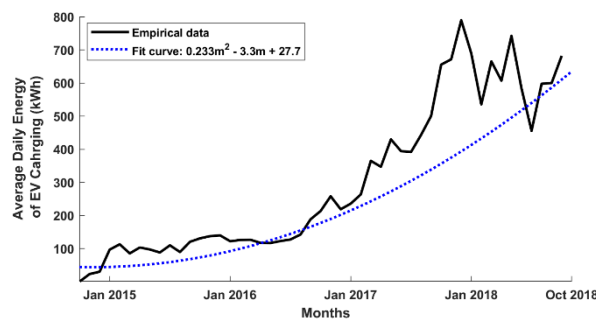


Figure 14: The average daily EV charging energy.

In order to predict the EV charging effect in the future, Figure 13 and 14 also show the fit curves using polynomial functions of order two. Table 3 lists the forecasting results of the monthly number of charging events and the average daily energy per month for 5 and 10 years using these fit curves. This table shows that if the EV growth continues at the same rate as in the last three years, it will need 10 times more energy in 10 years.

Table 3: The forecast of EV charging events' number and average daily energy in Helsinki area

	2018	2023	2028
EV charging events number per month	2162	10800	26266
EV charging daily average energy (kWh)	682	3005	7275

5.4 EV Flexibility

The flexibility model developed by equations (2)-(4) in Section II can define FCR-N flexibility profile of an EV charging event. Using this developed model, the FCR-N flexibility profile for all EV charging events in the Helsinki area are calculated.

The FCR-N flexibility density function can be calculated by aggregating all events of a day during the whole period. Figure 15 shows the cumulative density function (CDF) of the FCR-N flexibility that an EV could provide for each time interval (15 minutes). This CDF shows the probability for all the EV stations to provide flexibility (FCR-N) larger than a specific power.

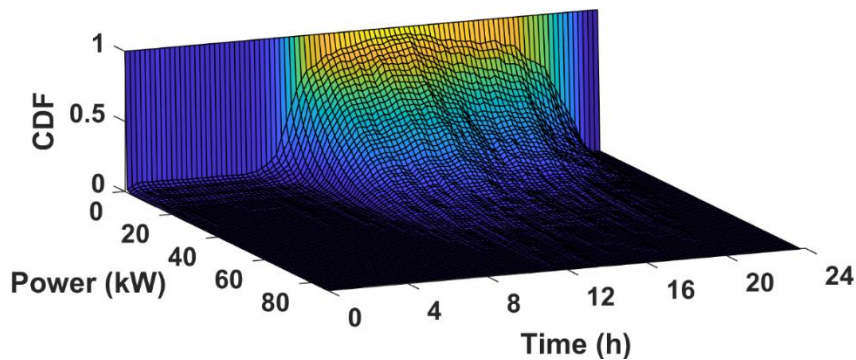


Figure 15: The cumulative density function (CDF) of FCR-N flexibility for different time of a day provided by EV.

Figure 16 depicts the expected value of the flexible power for FCR-N in the Helsinki area based on last year records. The most expected value for the flexibility of EV charging stations will be almost zero during the night and will be at a maximum of 16.74 kW at 2:00 p.m. It is important to notice that most of the stations included in the data are in public areas or on private companies premises where drivers charge their EV only during day times or working hours. It is the reason for the expected value of flexibility at night-time to be almost zero. Private car owners charging their car during the night do it almost exclusively straight from their electrical outlets instead of through a charging station. That charging does not appear in the available data.

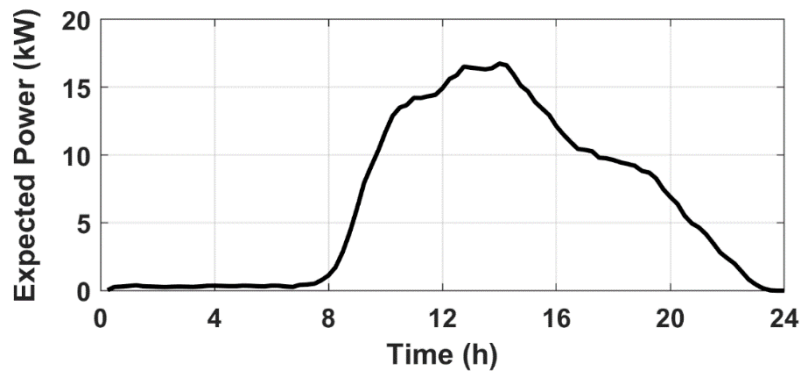


Figure 16: The expected flexibility (FCR-N) provided by EV charged in Helsinki area.

Although the EV charged in the Helsinki area cannot provide currently a considerable share of FCR-N need of Finland, they may be a more important source in the future. Figure 17 shows the flexibility growth of EV in Helsinki during the last three years. This monthly growth can be estimated by a second-order polynomial function, as shown in Figure 17. Using this linear fitting, the flexibility in 2028 (10 years later) is expected to be equal to 380 kW.

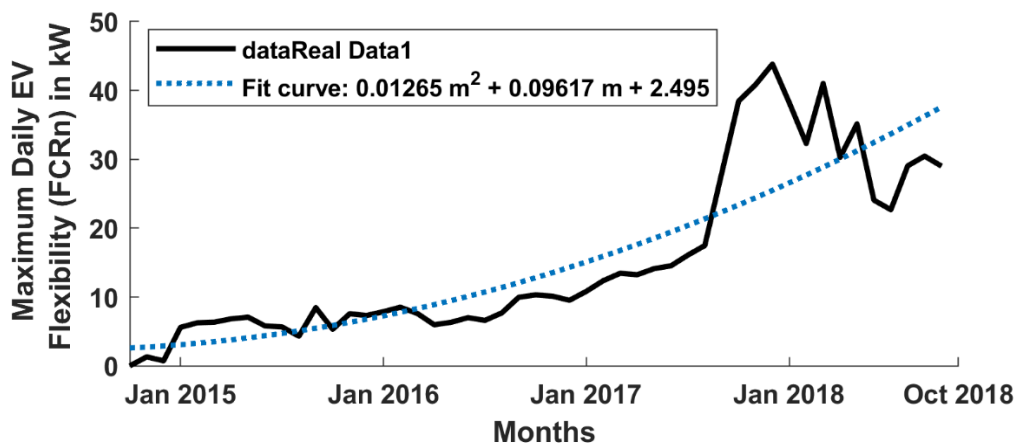


Figure 17: Flexibility (FCR-N) growth during the last three years.

6. Suvilahti: System Description

Suvilahti, an urban district in Helsinki, has become a site where new energy technologies are tested and where they can participate in the grid’s operation. In this study, of particular interest are battery energy storage (BESS), solar power plant, and an EV charging station located in Suvilahti. The BESS with a rated

power of 1.2 MW and an energy capacity of 0.6 MWh was installed to the site in August 2016, and ever since it has participated in power system operation, for example, by providing frequency controlled reserves and voltage support (Hellman et al. 2017). The BESS, shown in Figure 18, share the same connection point to 10 kV medium voltage network with the solar power plant. The plant has a nominal output power of 340 kW and its expected annual generation is approximately 275 MWh. These resources, the battery and the solar power plant, are owned by Helen Ltd. Furthermore, V2G charging stations, as well as a fast EV charging station, were installed in the same grid connection point. In September 2017, one 10 kW station with an ability to V2G was installed to the site and in 2018, a fast EV charger (50 kW) was installed. The V2G station and a glimpse from its opening event are presented in Figure 19.



Figure 18: Helen Ltd's energy storage in Suvilahti (Helen 2016)



Figure 19: V2G charging station in Suvilahti and its first charging (Picture: Helen Ltd)

The BESS is able to provide frequency controlled reserves, namely frequency containment reserve for normal operation (FCR-N) and frequency containment reserve for disturbances (FCR-D). In the Nordic power system, these reserves are responsible for continuous power balance maintenance since they follow the system frequency and are automatically activated. FCR-N aims to maintain the system frequency within normal operation range (49.9–50.1 Hz) so that the reserves are fully activated at the upper or lower limit of the range. They should be activated in 3 minutes and a dead band of +/- 0.05 Hz is allowed. The control of the reserves is based on a droop, which defines the output power as a function of the system frequency. Two examples are given in Figure 20, which depicts the droops tested with the battery in Suvilahti. In the figure, the droop utilized for FCR-D is also seen. FCR-D needs to be activated when the frequency falls below 49.9 Hz and it should be fully activated at 49.5 Hz. The activation time is defined so that 50% of the reserve is activated in 5 s and 100% within 30 s against a step-change in the frequency. Note that in the figure's case the droop is also applied between 50.1–50.5 Hz, which is not currently required.

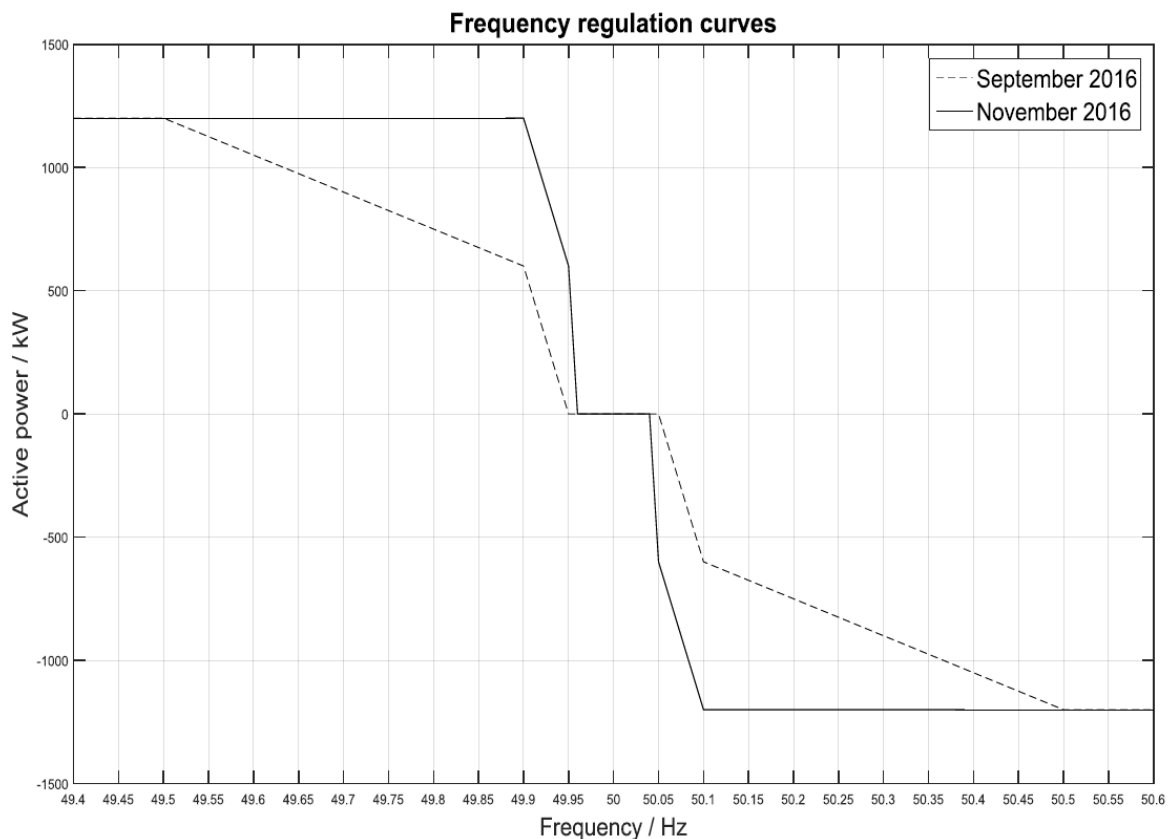


Figure 20: Frequency control droop of the BESS in Suvilahti (Hellman et al. 2017).

7. Investigated Control Strategies for Suvilahti

7.1 Aim of the strategies

This report has its focus on the EV charging. In a smart grid environment, the EV charging is commonly considered with other new resources, such as batteries and distributed generation, which is also the purpose here. The collaborative utilization of the BESS, PV generation, and EV charging is of particular interest when the control strategies are designed. Suvilahti is employed as a case study but it has some special characteristics, dictating the design and selection of the strategies. Firstly, the size of the PV and especially the storage's are considerably higher compared to the EV charging demand. Secondly, the BESS is likely to participate in profitable ancillary service provision due to its size and the investment cost that needs to be covered. Thirdly, the grid in Suvilahti is strong and thus, it is hardly affected by the studied resources.

Therefore, the strategies are designed in such a way that the BESS continues to provide frequency containment reserves, while its capacity is used to increase the utilization of solar energy in EV charging and in satisfying of other local electricity demand. The control strategies consist of the frequency control of the BESS and logics, which reduce the electricity exchange with the grid, increasing the use of PV for the charging and to cover the energy demand of the BESS (e.g. its losses). Three different frequency control strategies are investigated and they are further added with the logics. It is assumed that only the BESS is controllable, whereas the PV plant aims to maximize its generation and EVs simply aim to satisfy their charging demand. The assumption is made due to the fact that currently, the BESS is clearly the dominating resource at the site in terms of power and energy capacity. The strategies are described in the following section and related business cases are discussed in Section 7.4.

The reader should note that the investigated strategies are based on a heuristic approach. That is, they do not try to optimize the outcome but rather use a few parameters and real-time decision-making, which dictates the system's reaction to its inputs. The dominating input to the system is the system frequency, while the other inputs are the local PV generation and the charging load of a small EV fleet. All these inputs, particularly the frequency, are significantly difficult to forecast, complicating any approach relying on predictive decisions. By reducing the participation in frequency control, battery capacity would be available more for local PV and EV charging matching but this would inevitably reduce the monetary income.

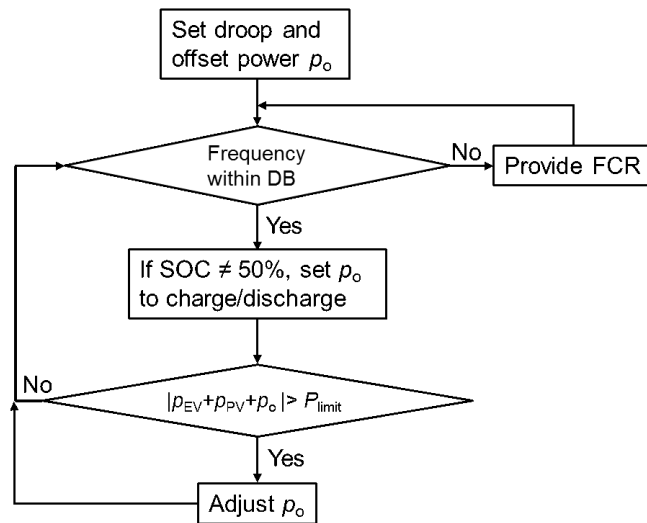
7.2 Exploiting the frequency control dead-band for the matching of local resources

This control strategy is based on the already tested frequency control approach of BESS in Suvilahti (Hellman et al. 2017). The BESS participates in the frequency containment process with the droop

depicted in Figure 20. Thus, a part of the power capacity is reserved for FCR-N and a part for FCR-D. The oscillating and biased system frequency naturally causes the battery to charge or discharge, which may empty or fully charge the battery. This prevents the battery to provide the reserves as it cannot charge or discharge anymore. Therefore, once the frequency is within a dead-band and frequency regulation is not provided (± 0.05 Hz from the nominal 50 Hz), the battery starts to charge or discharge with constant power (offset power) until it reaches 50% state of charge or the frequency regulation is again needed.

As stated earlier, all the resources are connected to the distribution grid at the same point. The utilization of local resources for the EV charging is thus improved if the energy is not drawn from the grid. Similarly, the utilization of PV generation is improved if excess power is not injected to the grid. By avoiding import or export of electricity, the utilization of local resources can be increased, which is the rationale behind the proposed control strategies. For the control, maximum allowed import and export powers are defined. These power limits are applied only when the frequency is within the dead-band and the frequency regulation is not needed. The control strategy is given as a flow chart in Figure 17. The reader should note that neither FCR nor the matching of local generation and consumption can be properly provided if the battery is full or empty, i.e., BESS charging is not possible if the battery is full and discharging is not possible if it is empty.

Based on the flow chart presented in Figure 21, the first task is to set the droop and the offset power, p_o . That is, the droop defines the amount of power provided for FCR-N and FCR-D. An example of a droop is given in Figure 20. The offset power defines the power that is used to maintain SOC near the middle point (50%) and that is exploited to limit the electricity export and import. Next in the figure, a decision is made whether to a response to the frequency is needed or the offset power is activated to charge or discharge the battery. The system also needs to monitor if export or import limit, P_{limit} , is violated, i.e., the sum of PV generation, EV charging, and the offset power exceeds the limit. In such a case, the offset power is adjusted (increased or decreased).



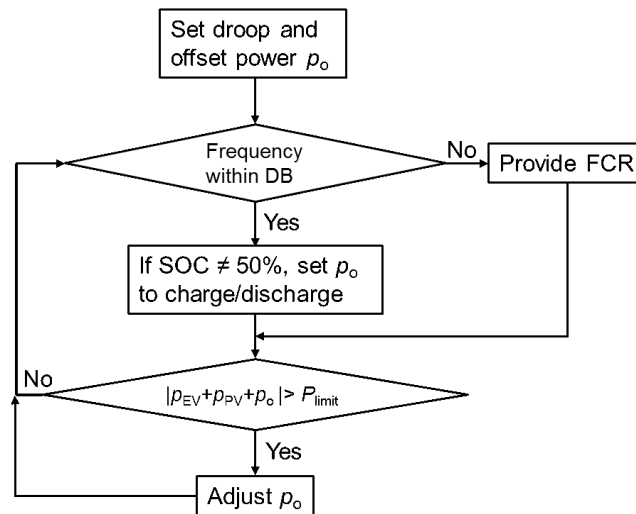
p_o is the offset power, DB is the dead-band, p_{EV} is the EV charging load, p_{PV} is the PV generation, P_{limit} is the allowed import/export power.

Figure 21: Control strategy to provide FCR and to match local consumption and generation when the frequency is within the dead-band.
In the figure

7.3 Exploiting a part of the BESS’s power capacity for the matching of local resources

The strategy defined in the previous section assumed that the full power capacity of the BESS is reserved for FCR and local balancing is performed only if the frequency is within the dead-band. As an alternative, this section considers strategies that divide the power capacity into two: a major part is reserved for the FCR and the rest for local matching. This naturally reduces the reserve provision but enables continuous local balancing. Two strategies will be considered.

Firstly, Figure 22 introduces a strategy closely related to the one described in Section 7.2. The difference is the power, p_o , which can be continuously used for local matching. This same power is also used to charge or discharge the battery if the frequency is within the dead-band and SOC deviates from 50%.



p_o is the offset power, DB is the dead-band, p_{EV} is the EV charging load, p_{PV} is the PV generation, P_{limit} is the allowed import/export power.

Figure 22: Control strategy to provide FCR and to match local generation and consumption with the offset power. SOC is targeted to be 50%.

The second strategy relies on the BESS control, which is previously studied and applied, for example, in (Megel et al. 2013) and (Alahäivälä & Lehtonen 2016). The strategy divides the power capacity of the BESS into reserve power and offset power, p_o . The offset power is used to maintain the SOC of the battery between predefined upper and lower SOC limits. Therefore, if the SOC exceeds the upper limits, the battery starts to discharge itself with a power of p_o . The discharging is activated for a time period of t_0 , which is also defined in advance. Similarly, if the SOC falls below the lower limit, the charging power of p_o is activated for the time period of t_0 . The offset power is also utilized for the local matching if import or export power exceeds the set limits. The control strategy is given as a flow chart in Figure 23, where

Firstly in the flow chart, the droop for the FCR participation is defined and the SOC limits (\underline{SOC} and \overline{SOC} , lower and upper SOC limit), the offset time, t_0 , and the offset power, p_o , are set. Secondly, the BESS starts to provide FCR based on the defined droop. If the battery SOC exceeds the limits, the offset power is activated. The system also continuously monitors whether the import or export limits are violated and adjust the offset power if required. One can note that several parameters need to be defined for the strategy but there is no simple rule on how to select the values. Instead, historical data and system simulation can assist in finding the optimal parameter values. One example can be found in (Alahäivälä & Lehtonen 2016), where the studied BESS is simulated with a vast number of control parameter values. The optimal values maximize the amount of provided power for FCR, while the battery should not become full or empty during the control. In addition, all the proposed strategies could be possible to implement using net load, which is the sum of PV generation and EV charging load. Thus, the import for EV charging

or export of PV generation could be prevented, while frequency control-related offset power could be activated if the SOC level needed to be maintained. This notion becomes particularly important to consider if the power limit is set to be quite low. The BESS cannot provide FCR well without an ability to activate the offset power.

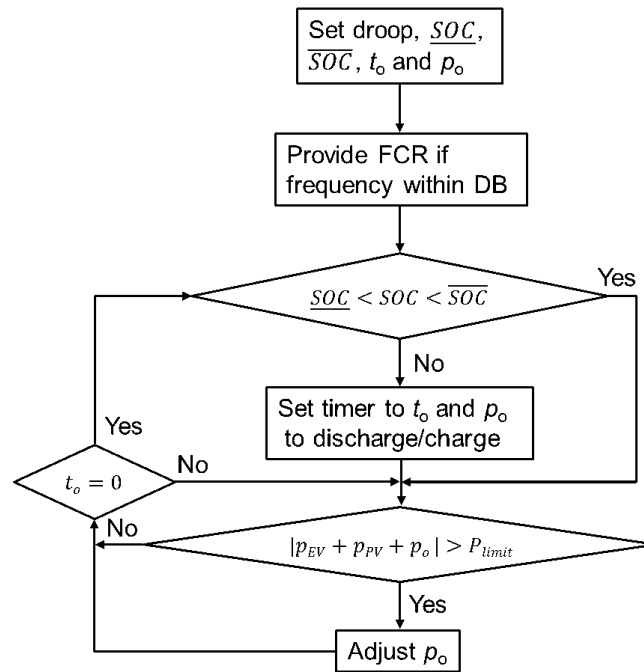


Figure 23: Control strategy to provide FCR to match local generation and consumption with the offset power.

7.4 Potential as a business case

The described control strategies assume that a single entity owns the BESS, the solar power plant, and the EV charging stations. It is also the actor that uses the resources to maximize its profit. The operational costs within the strategies are due to the electricity procurements for the EV charging and the BESS’s offset energy as well as possible maintenance cost of the system. Income, on the other hand, can be received from the selling of PV generation, reserves, and other possible ancillary services, such as reactive power compensation if a local DSO reactive power market or a bilateral contract with the DSO existed. Nevertheless, one should note that the selling price of PV generation needs to be lower than the buying of electricity in order for the strategies to be reasonable.

For the practical implementation of the strategies, a power measurement of the electricity import and export is required at the point of connection to the distribution grid. A controller able to adjust the BESS power is also required in a case if the power measurement indicates the violation of the export and import limits. One can also note the export and import limits can be dynamically adjusted, for example, depending on the forecasted PV generation for the next day.

8. BESS Simulation Studies on the Strategies

8.1 Aim of the simulations

The simulations are performed in order to test the control strategies proposed in Section 7. The operation of the strategies is first visualized, after which their performance is evaluated with several measures that are:

- Influence of the strategy on the electricity import and export, i.e., how well the battery is utilized for the matching of local load and generation
- Degree of energetic self-supply by PV, i.e., the percentage of the local consumption supplied by the PV.
- Influence of the strategy on the maximum import and export powers
- Performance of the battery, i.e., the time it is nearly full of empty.

8.2 Simulation setup and simulated cases

The simulation setup consists of input data, a simplified dynamic BESS model, and the control algorithms that are implemented in Matlab. The input data includes measured power system frequency, the measured generation of Suvilahti solar power plant, and simulated EV charging load. The simulation of the strategies is performed over a two-month period (August and September in 2016) with one second time resolution. The frequency and generation data are from this period and they are depicted in the case of an illustrative week in Figure 24 and Figure 25, respectively.

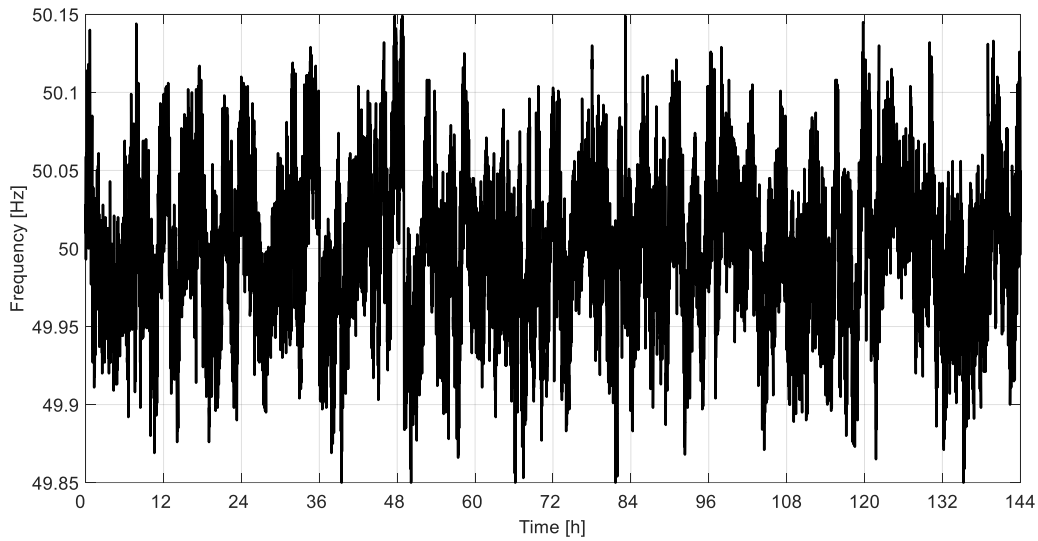


Figure 24: System frequency for an illustrative week in August 2016.

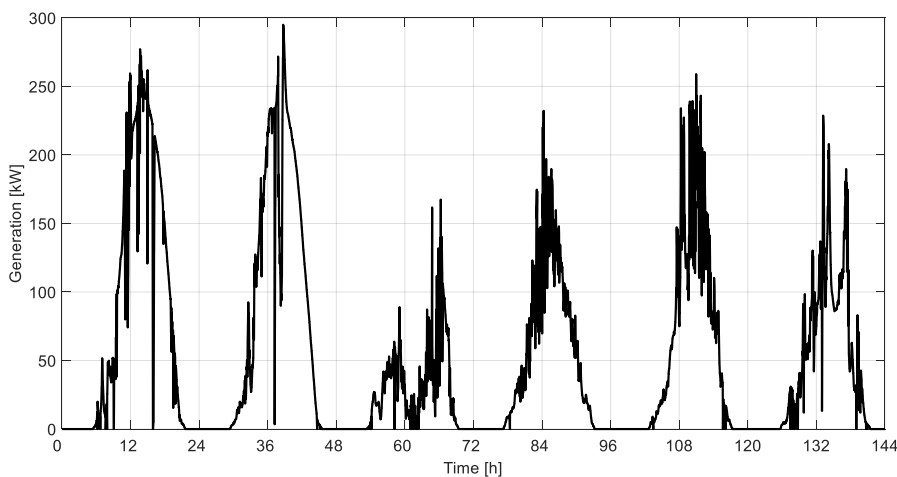


Figure 25: The generation of the Suvilahti solar power plant for one week in August 2016.

Since there is no historical EV charging load data from Suvilahti, it is constructed by the Monte Carlo simulation model presented in (Alahäivälä 2012). The model employs the mobility data of the Finnish National Travel Survey, which offers information on the typical travelled distances by passenger cars and the starting times of different trips. This data together with a simple EV model (travelling speed, battery size, consumption per kilometre, charging power and efficiency) and the Monte Carlo method can be used to simulate the daily driving behaviour of an EV. When the EV is parked, it can be assumed to charge with a predefined power until the battery is full or the car departs. The Monte Carlo method randomizes the trip starting times and distances based on the input data and therefore, every simulation iteration produces a unique charging profile. The model enables trips to different destinations, including trips to the workplace, public places, and home. Suvilahti is assumed to be a location where working place and public place

related charging occurs. It is further assumed that there lie 20 charging stations with a charging power of 25 kW per charger at the site. Further, a case with 100 stations is included in the simulations for comparison. The charging profile of a random weekday is given in Figure 26 in the case of the 100 charging stations. The figure also illustrates the average (average over several random days) charging load on a weekday and weekend. During a single day, the charging profile seems somewhat random and high power peaks can occur. However, the average profiles indicate that the charging load peaks can be expected to occur between 8-9 in the morning and later between 16-18 in the evening.

The EV charging load for the two-month period (20 charging stations) is approximately 5 MWh with a peak power of 100 kW. For the 100 charging stations the consumption is approximately 27 MWh with a peak power of 275 kW. The PV generation for the same period is 57 MWh with a maximum generation of 295 kW.

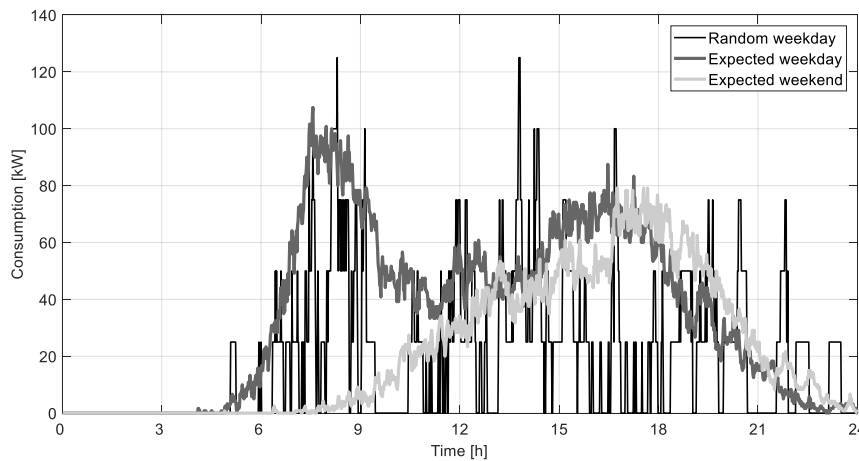


Figure 26: EV charging load of 100 stations. The figure shows a randomly selected weekday and the expected charging profiles for a weekday and weekend day.

The dynamic BESS model is represented by the following equations:

$$SOC_{k+1} = SOC_k - \frac{\Delta k}{E} \begin{cases} \frac{1}{\eta_d} p_k, & \text{if } p_k > 0 \\ \eta_c p_k, & \text{otherwise} \end{cases} \quad (6)$$

where k is the time step, Δk is the length of the time step (1 second), E is the storage energy capacity (600 kWh), η_d and η_c are the discharging and charging efficiencies (assumed to be 90%), respectively. p is the charging/discharging power and it is given by

$$p_k = p_k^{FCR} + p_k^o \quad (7)$$

where p^{FCR} is the activated reserve power and p^o is the activated offset power (the same as p_o defined earlier in the report). The power is bounded by the BESS power capacity 1.2 MW. The presented model is basically to say that during each time step, the charging/discharging power of the BESS is first evaluated based on the strategies described in Section 7 and then the SOC for the next time step is solved.

The simulations consist of five base cases (Cases 1–5) which correspond to the described control strategies with and without the import/export limitations. These cases are also simulated with different parameter values, that is, with different export/import limits and the number of EV charging stations. In all the cases, the frequency control dead-band and the frequency range of the reserves are as defined in Section 4 and in Figure 20. The cases from one to five are:

- Case 1: the control strategy presented in Figure 21 when FCR-N power is 600 kW, FCR-D power is 600 kW, and offset power is 200 kW. There is no export/import limits.
- Case 2: the same as Case 1 but the export and import limits are set to 200 kW.
- Case 3: the control strategy presented in Figure 22 when FCR-N power is 600 kW, FCR-D power is 500 kW, and offset power is 100 kW. The export and import limits are set to 200 kW.
- Case 4: the control strategy presented in Figure 23 when FCR-N power is 600 kW, FCR-D power is 500 kW, and offset power is 100 kW. There is no export/import limits.
- Case 5: the same as Case 4 but the export and import limits are set to 200 kW.

For the cases 4 and 5, the upper and lower SOC limits are 70% and 30%, respectively, and the offset power is activated for 30 minutes if the limits are violated. Case 1 corresponds to the strategy that has already been tested in Suvilahti and reported in (Hellman et al. 2017). Note that it is the business as a usual case where import and export are not limited and the BESS merely participates in the frequency control. In order to provide some validation to the simulation, Figure 27 and Figure 28 compare measured and the simulated behaviour of the BESS's state of charge during a period of one and half days in September 2016.

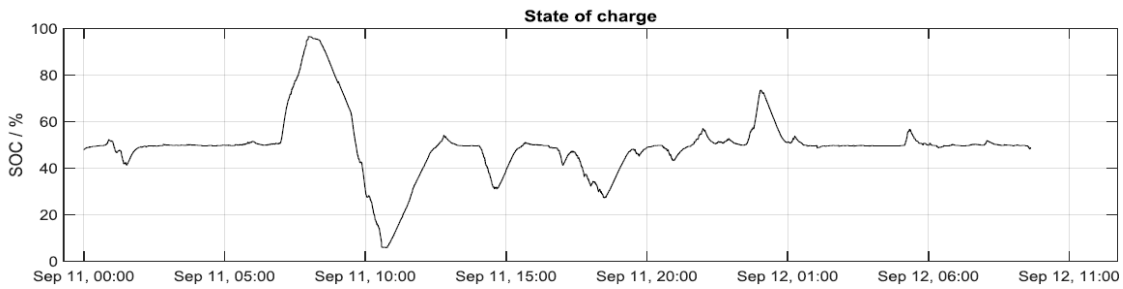


Figure 3: The state of charge of the BESS on September 11th and 12th, 2016.

Figure 27: Measured SOC of the BESS (Hellman et al. 2017).

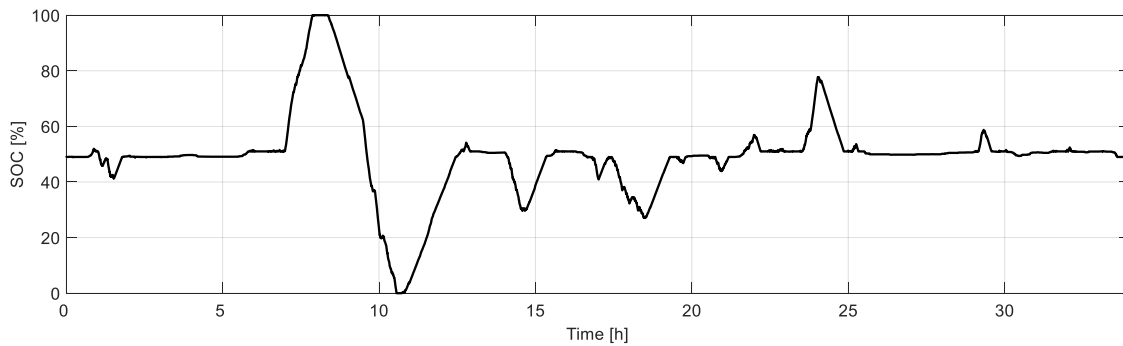


Figure 28: Simulated SOC of the BESS. This is a snapshot from the simulation run over the two-month period (August and September 2016).

8.3 Results

8.3.1 Comparison of the control strategies

This section first showcases the operation of each strategy using a two day period (August 2 and 3, 2016) as an example. Each figure from Figure 29 to Figure 33 contains four subfigures, depicting the consumption and generation at the site (EV charging, PV generation, and the offset power of the BESS), the net load of the site (the sum of the previous three. Export is positive and import negative), activated FCR including FCR-N and FCR-D, and the SOC of the BESS.

Based on the figures, the following observations can be made. Firstly, it can be seen that the charging load of 20 stations is significantly lower than the BESS’s offset power and PV generation. Nevertheless, the charging coincides well with the PV generation. Secondly, when the cases from 1 to 3 are compared with the cases 4 and 5, the first three cases maintain the SOC closer to the 50%, whereas the SOC varies more in the cases 4 and 5. This is due to the control strategies and the approach they use to maintain the SOC level near the middle point. Consequently, the offset power is required repeatedly with the cases from 1 to 3 and only occasionally with 4 and 5. Thirdly, the use of export limit clearly cuts the peak generation of the solar power plant, i.e., the peak generation around midday is stored to the battery. The limiting of import cannot be seen in the figures because of the high 200 kW limit. Fourthly, the activated

FCR varies approximately between -600 kW and 600 kW. The net load (the sum of EV charging, PV generation, and the offset power of BESS) can also reach nearly these values if the limiting is not in use as seen especially in Figure 29.

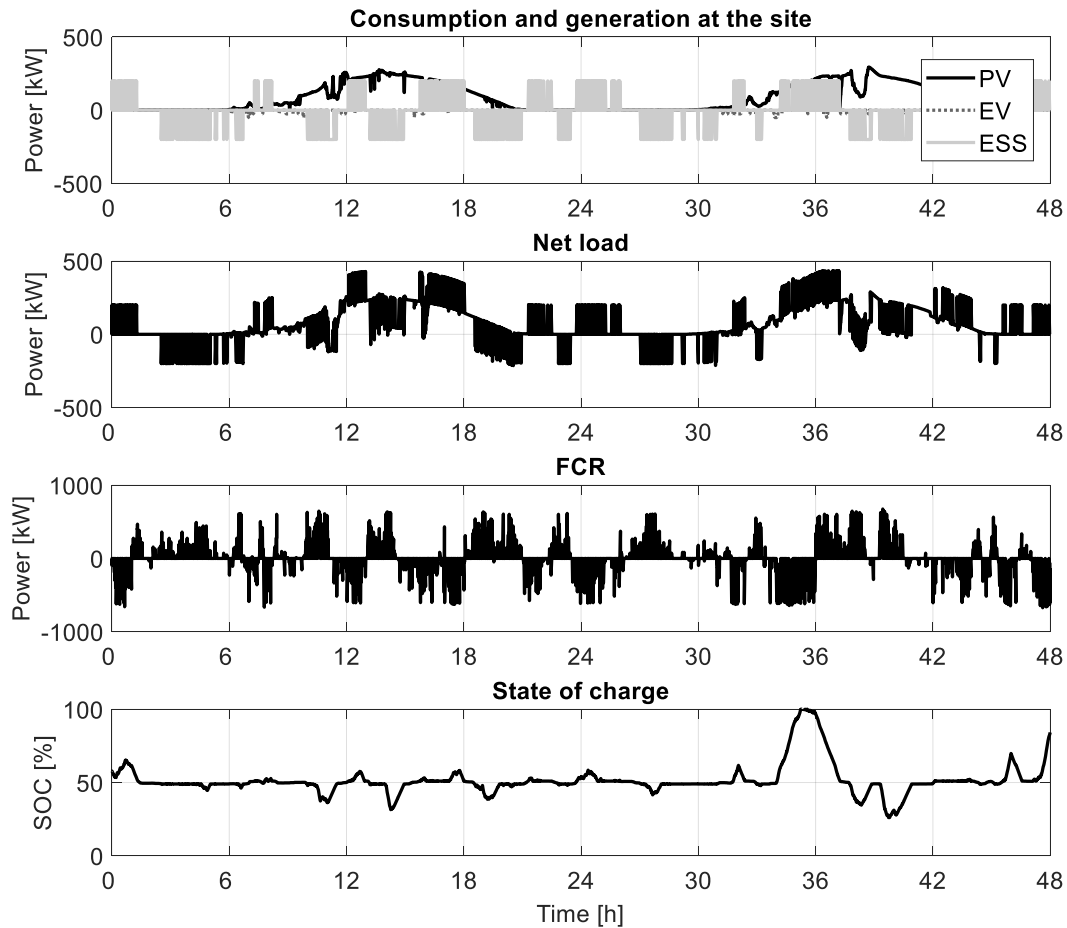


Figure 29: Illustration of Case 1 over a two-day period. In the uppermost subfigure, ESS indicates the offset power of the BESS. The net load is the sum of PV generation, EV charging, and the offset power. FCR is the activated reserve power by the BESS. Its SOC is depicted in the lowest figure.

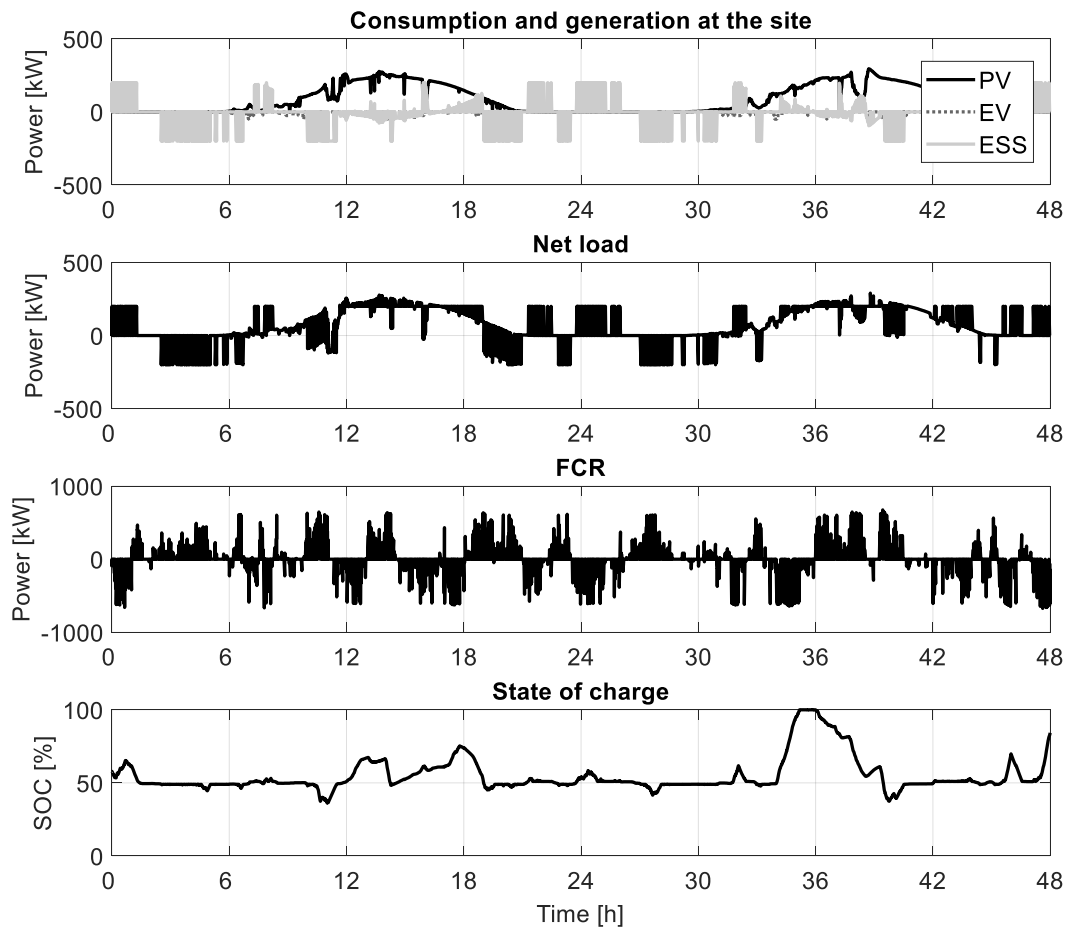


Figure 30: Illustration of Case 2 over a two-day period. In the uppermost subfigure, ESS indicates the offset power of the BESS. The net load is the sum of PV generation, EV charging, and the offset power. FCR is the activated reserve power by the BESS. Its SOC is depicted in the lowest figure.

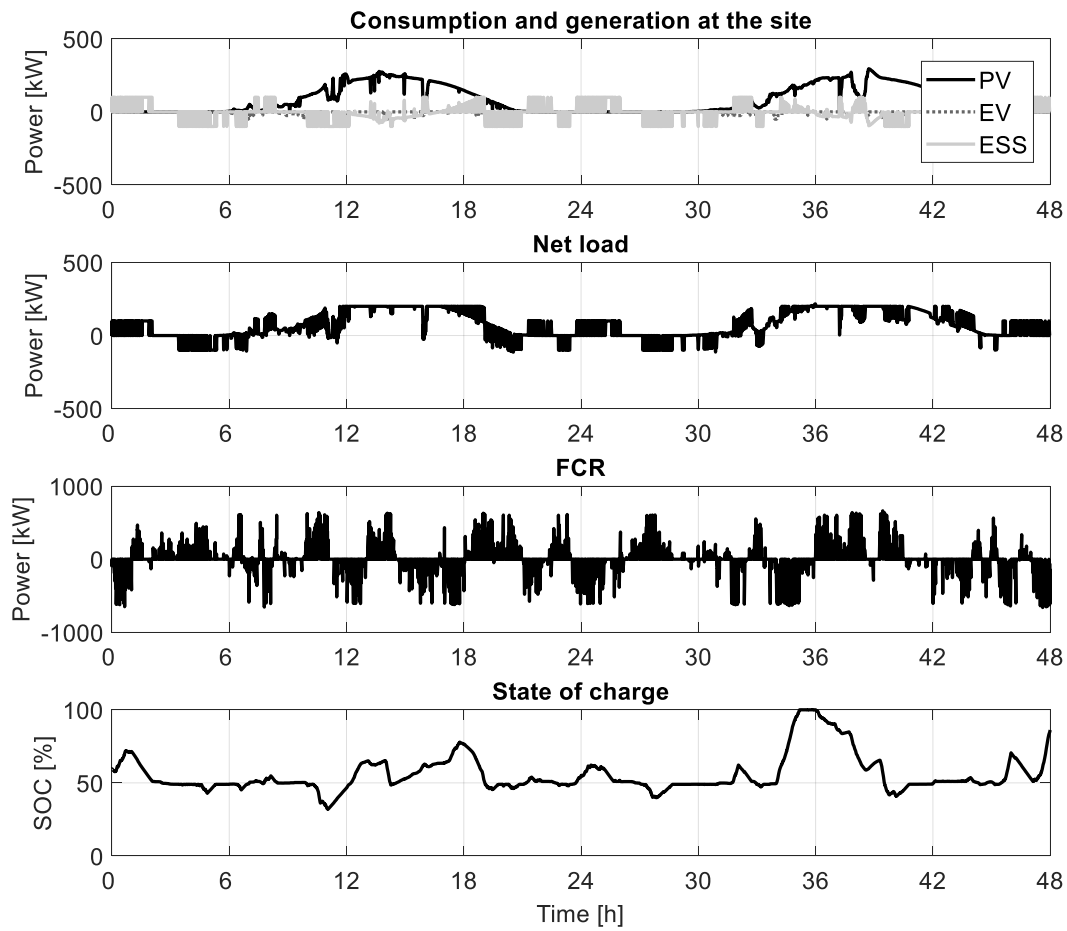


Figure 31: Illustration of Case 3 over a two-day period. In the uppermost subfigure, ESS indicates the offset power of the BESS. The net load is the sum of PV generation, EV charging, and the offset power. FCR is the activated reserve power by the BESS. Its SOC is depicted in the lowest figure.

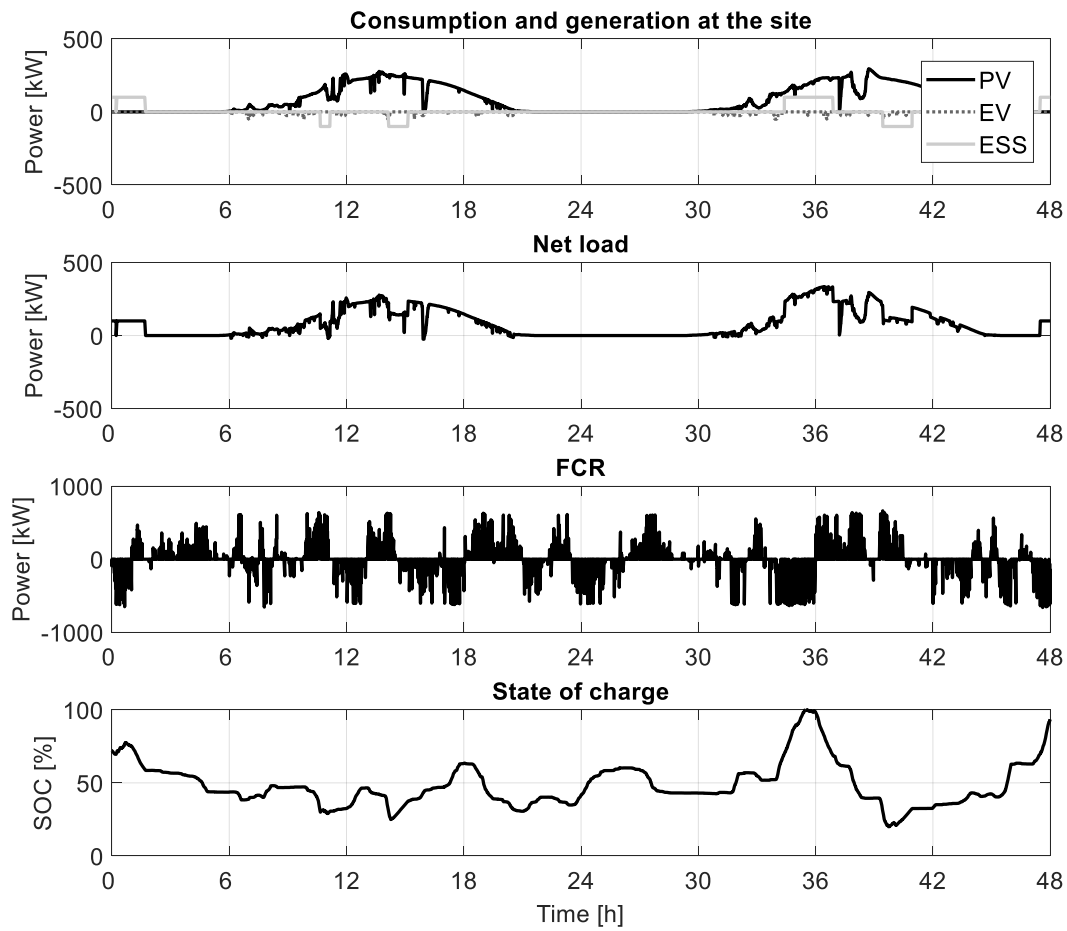


Figure 32: Illustration of Case 4 over a two-day period. In the uppermost subfigure, ESS indicates the offset power of the BESS. The net load is the sum of PV generation, EV charging, and the offset power. FCR is the activated reserve power by the BESS. Its SOC is depicted in the lowest figure.

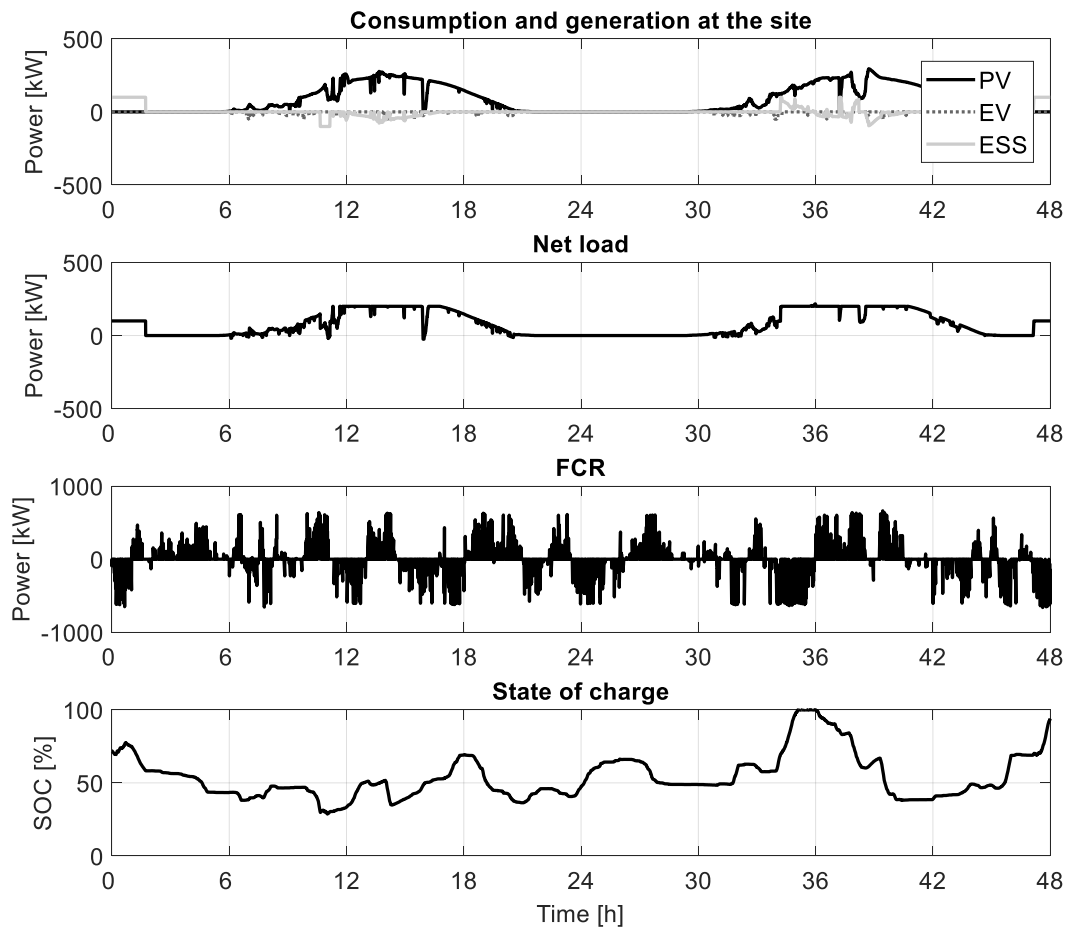


Figure 33: Illustration of Case 5 over a two-day period. In the uppermost subfigure, ESS indicates the offset power of the BESS. The net load is the sum of PV generation, EV charging, and the offset power. FCR is the activated reserve power by the BESS. Its SOC is depicted in the lowest figure.

The following compares the cases in terms of imported and exported energies, maximum import and export powers, and the percentage of the time the battery is nearly full or empty. All the values are calculated over the simulated two-month period. Based on Figure 34, exporting occurs more in general, which is due to the PV generation. Case 5 shows the lowest energy exchange with the grid among the cases but the difference between cases 4 and 5 is minor. The lower exchange compared to cases from 1 to 3 is likely caused by the control logic, which aims to keep the SOC between 30% and 70%. Thus, SOC can vary quite freely and less offset power is required. When interpreting the figure, one should remember that the PV generation during the period is 57 MWh (causes export) and the EV charging load 5 MWh (causes import). In addition to these, the offset power of the BESS causes import and export. When the Degree of energetic self-supply by PV is considered for the cases from 1 to 5, the values are 26%, 25%, 37%, 39%, and 36%, respectively. Better results are clearly achieved when the battery power capacity is

divided into the offset power and the power for frequency control. In the case of Case 4 and Case 5, the consumption is lower compared to the cases from 1 to 3, which consequently improves the self-supply.

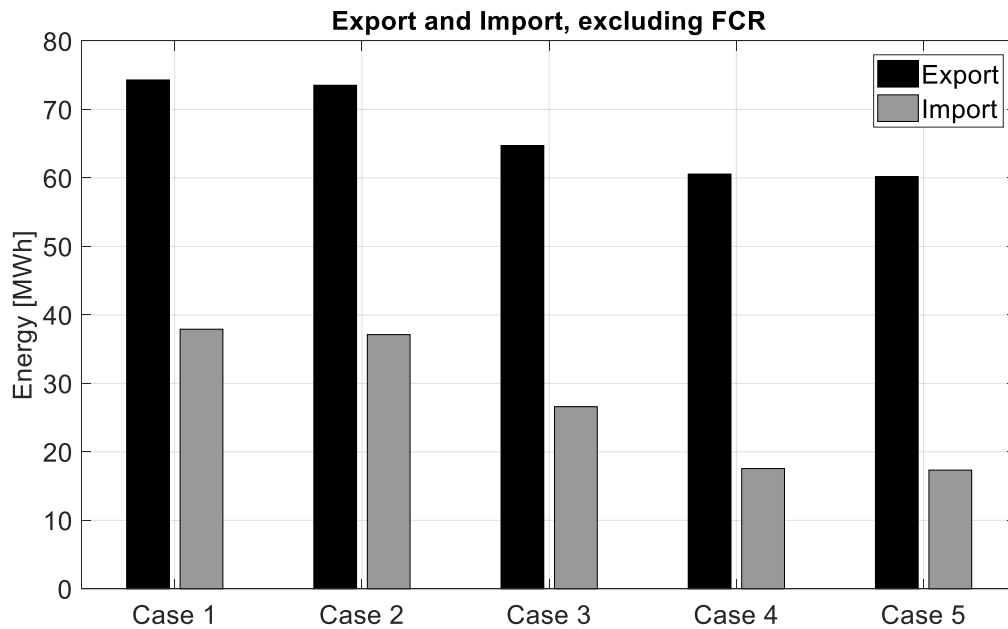


Figure 34: The exported and imported energies during the simulation period. The values contain only PV generation, EV charging, and the offset power of the BESS. That is, the energy needed for FCR is not included.

Figure 35 visualizes the maximum export and import powers of the net load during the simulation period. The cases (Case 2, Case 3, Case 5) that aim to limit the export and import to 200 kW clearly reduces the maximum export power. The imported power is naturally less than the limit so Case 1 increases the import power. However, the reader should note that the BESS provides a reserve power of 1.2 MW for FCR, which is a significantly higher power than it can be seen in Figure 35. Thus, in Case 1 and Case 2, the maximum exporting power is the sum of FCR activation and PV generation (1.2 MW plus 340 kW), whereas for Case 4, it is the sum of FCR activation, the offset power, and PV generation (1.1 MW plus 100 kW plus 340 kW). In Case 3 and Case 5, the maximum FCR is 1.1 MW but the offset power, 100 kW, can be activated to reduce the export of PV to 240 kW if it generates its rated output.

The purpose of Figure 36 is to assess the ability of the control strategy to maintain the BESS operational, that is, to prevent the battery to become fully charged or empty. All the data points with a SOC value over 95% or below 5% are considered to nearly full or empty in the presented graphics. For most of the cases, the battery is nearly full or empty approximately 1.5% of the time during the two-month period. In Case 3, the corresponding value is approximately 3%.

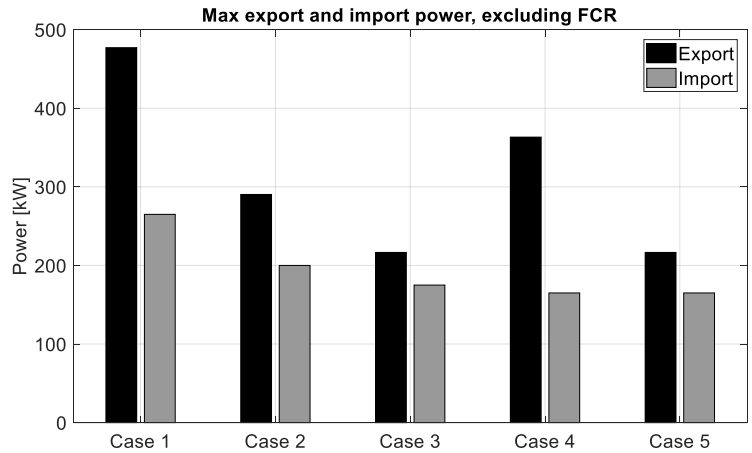


Figure 35: The maximum export and import powers during the simulation period. The values contain only the sum of PV generation, EV charging, and the offset power of the BESS, i.e., the net load.

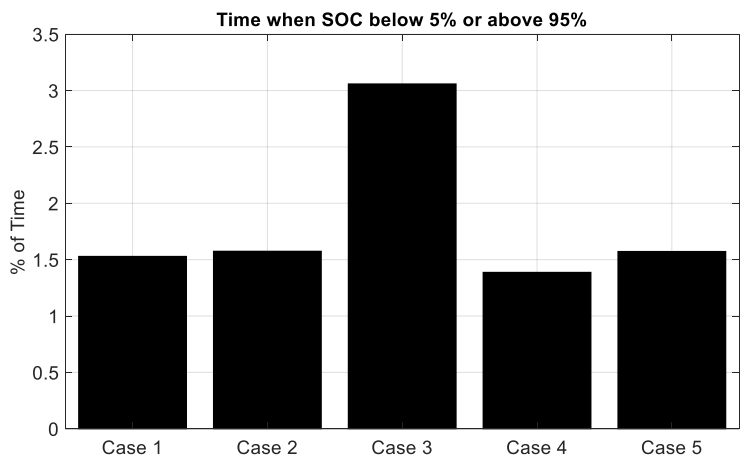


Figure 36: Percentage of time when the battery is nearly full or empty during the simulation. For example, 1% is approximately 14 hours (the studied period is two months).

8.3.2 Sensitivity analysis

A sensitivity analysis is performed in this section to open the influence of the import and export limits on the energy import and export in Figure 37 as well as on the time the battery is nearly full or empty Figure 38. The analysis is done with 20 (Figure 37 and Figure 38) and 100 EV (Figure 39 and Figure 40) charging stations. Only cases 2, 3, and 5 are considered as the power limits are not used in cases 1 and 4. Generally, the task of setting the export and import limits is to find a trade-off between energy exchange with the grid and the ability of the BESS to remain operational. For example, energy import can be prevented by setting the import limit to zero but this will consequently cause the battery to remain nearly full or empty approximately 12% of time as seen in Figure 38. More realistic limit values would be from 50

to 100 kW for import and 150 kW for export. This would reduce the energy exchange with the grid compared to the base cases studied in the previous section while the BESS would still be able to provide FCR more than 96% of time.

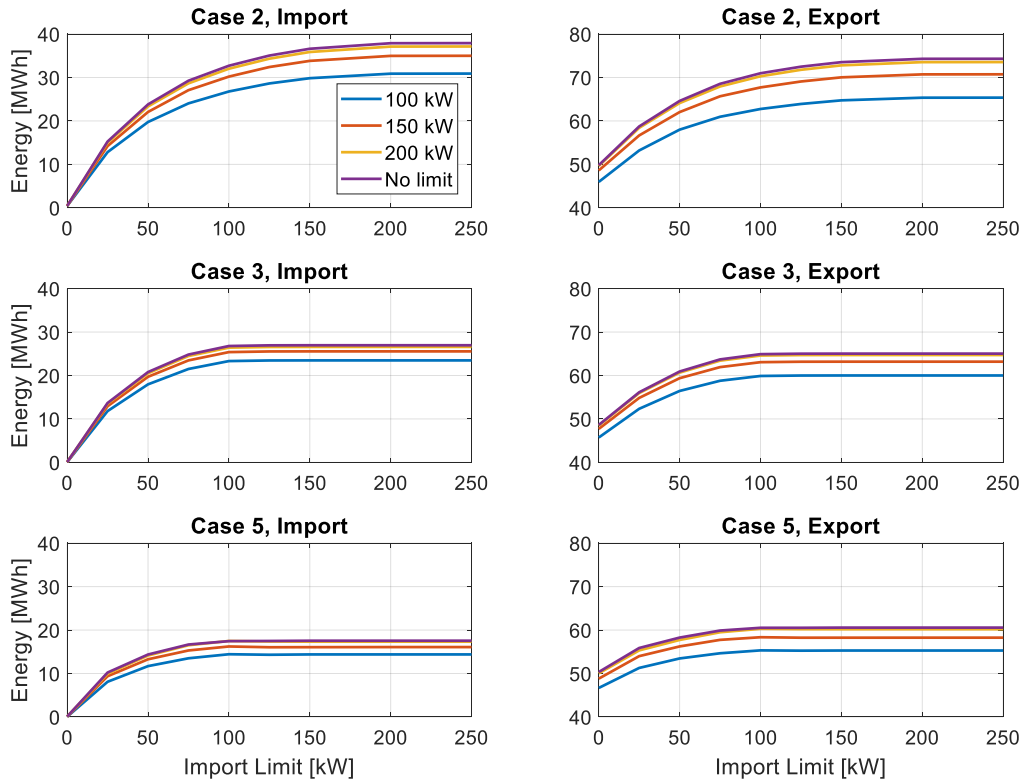


Figure 37: The sensitivities of the energy import and export on the import limits (x-axis in the subfigures) and export limits (different lines in the subfigures) with 20 EV charging stations. The limits are only used with cases 2, 3, and 5 so they are shown in the figure.

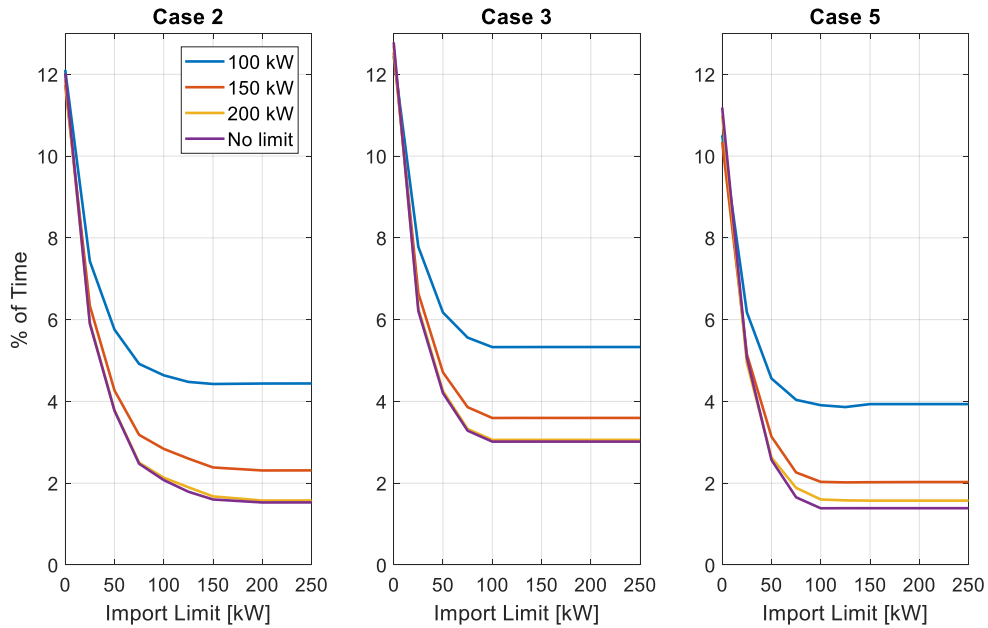


Figure 38: Percentage of time when the battery is nearly full or empty and its sensitivity on the import limits (x-axis in the subfigures) and export limits (different lines in the subfigures). 20 EV charging stations.

If the number of the charging stations is increased to one hundred, the system needs to start importing even though the import limit is set to zero. It can generally be seen in Figure 39 that the energy import increases approximately by 10 MWh compared to the cases with 20 charging stations. On the other hand, the amount of exported energy decreases by approximately 10 MWh. This is to say that a greater portion of the PV generation is utilized locally but the local demand exceeds the available local resources more often. Further, it should be noted that the offset power of the BESS in cases 3 and 5 is only 100 kW while the EV charging load peak can be higher. Based on

Figure 40 the export limit can now get lower values and the BESS still remains operational (less than 4% of time nearly full or empty).

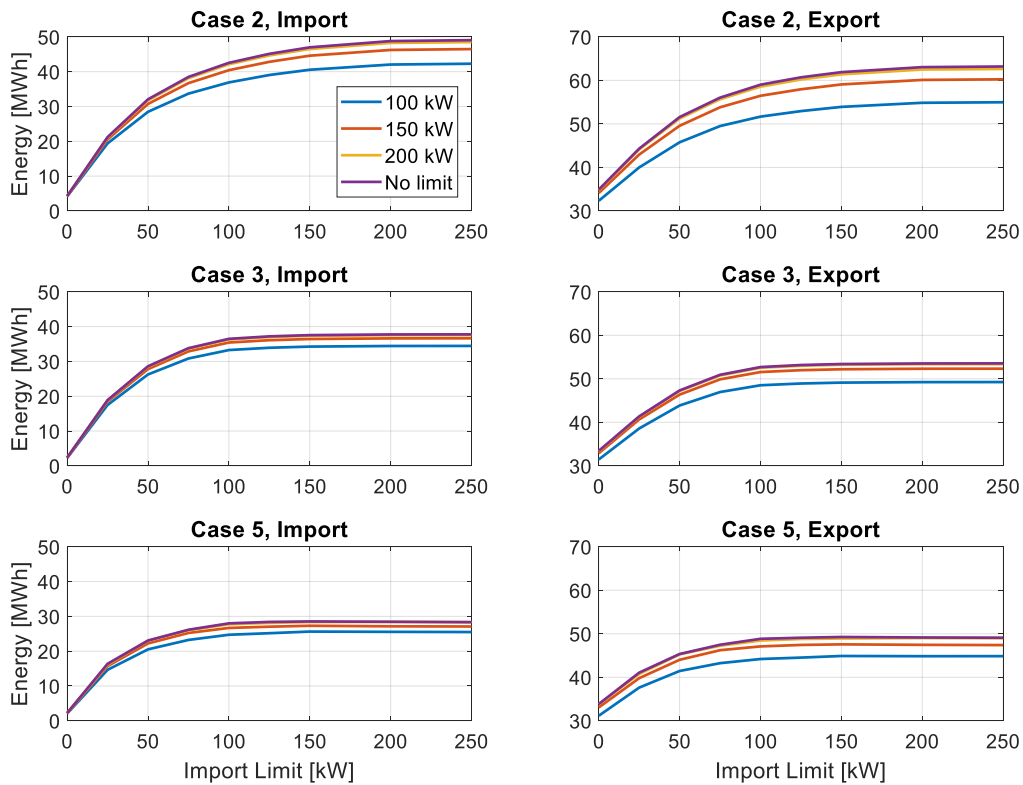


Figure 39: The sensitivities of the energy import and export on the import limits (x-axis in the subfigures) and export limits (different lines in the subfigures) with 100 EV charging stations. The limits are only used with cases 2, 3, and 5 so they are shown in the figure

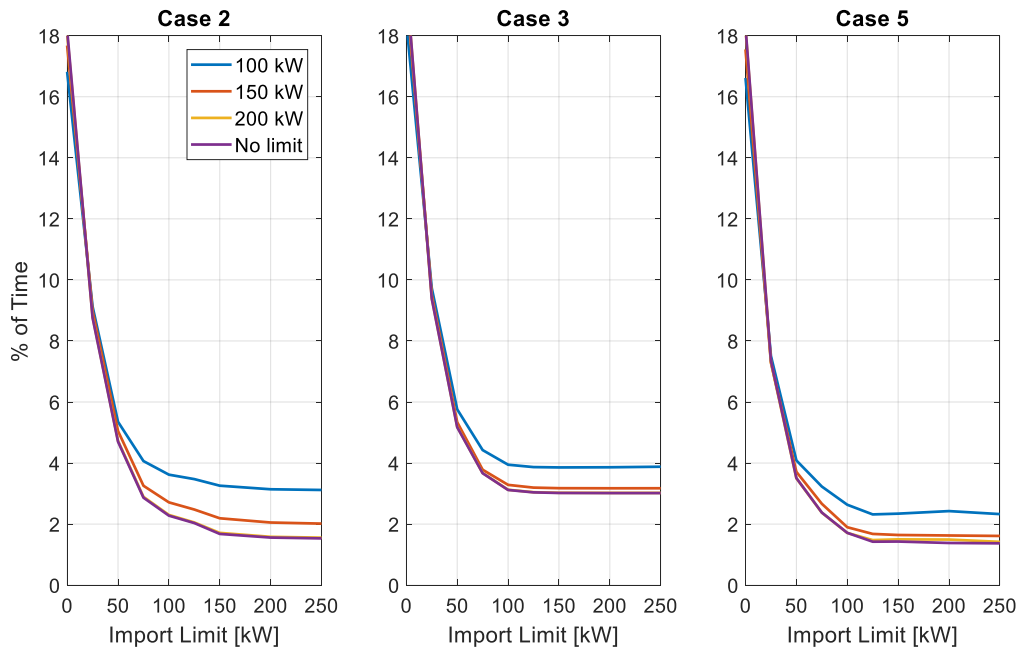


Figure 40: Percentage of time when the battery is nearly full or empty and its sensitivity on the import limits (x-axis in the subfigures) and export limits (different lines in the subfigures). 100 EV charging stations

8.3.3 Result Summary

The following core observations can be made from the presented results

- Case 1 and Case 2 allow the BESS to provide its whole power capacity for FCR since the offset power is activated only when the frequency is within the dead-band. This, on the other hand, results in an intermittent offset power usage and reduced ability to limit the export-import power in Case 2 (no limit is forced in Case 1).
- Case 3 reduces the energy import and export effectively and limits the power well. Nevertheless, the control strategy has difficulties to prevent the fully charging or discharging of the battery.
- Case 4 and Case 5 indicate the best reduction in energy export and import. They also reduce the intermittency of the offset power usage. However, a part of the battery power capacity needs to be reserved for the offset power, which reduces income from the FCR provision.
- Export and import power limits can be used to reduce energy import and export (better matching of local consumption and generation) but strict limits easily result in an empty or fully charged battery.

9. Demonstrations in Suvilahti

This chapter focuses on the different types of demonstrations done by Helen with the assets in Suvilahti. The main focus of the chapter is on the demonstrations done with the Suvilahti Battery energy storage system (BESS) but also a performance test with the V2G charger in Suvilahti is described. Chapter 9.1 presents the results of frequency control tests, metro peak shaving, reactive power and voltage control tests done with the BESS. Chapter 9.5 gives a description of three control tests done with the Suvilahti V2G charger.

9.1 Demonstrations of Suvilahti BESS

Suvilahti Battery energy storage system has provided a research platform for Helen for three years since August 2016. The purpose of purchasing the battery was to demonstrate the multi-functionality of the battery and its technical capability to provide services for several stakeholders. The starting point was that the BESS was first of its kind and applicability to different services was undefined in reality even though the topic was already much discussed in articles. To learn the best practices from the operating environment, its limitations and make a change to the regulation, also local DSO Helen Electricity Network and Finnish TSO Fingrid participated in the research project of Suvilahti BESS.

The main research questions were how to provide ancillary services to TSO, such as reserve power in FCR-N market, how to implement peak power shaving and energy time-shifting for the DSO's needs such as smoothing out PV production, shaving dynamic office electricity consumption loads and shaving the metro acceleration and braking peak powers from neighboring substation. The local DSO also needs voltage and reactive power control in their distribution grid and they are responsible for controlling reactive power and keeping it within a PQ-window set by the TSO. During the research phase, the BESS has also been providing voltage control and reactive power compensation services.

All of the studied cases have helped in defining suitable business cases to Helen's customers. Different customer segments have different needs, but it is typical that the battery is not fully utilized by the customer. Part of the time the battery capacity could be used as a reserve asset to provide services e.g. to TSO or maybe someday also to the DSO. The research project has given insight into the business models how Helen offers the solution to its customers. The customers can purchase battery storage systems from Helen based on a 10-year contract with fixed monthly fee or with their own investment. Helen's customers can become a part of Helen's virtual power plant, which means that the storage solutions have built-in capability to provide ancillary services to TSO reserve market with commonly agreed times.

Suvilahti BESS is used to demonstrate multiuser applications, which include:

- Reserve power for the Fingrid Oyj (Transmission system operator)
- Peak power shaving for the Helen Electricity Network (Distribution system operator in Helsinki)
- Energy time-shifting for the Helen Electricity Network
- Voltage support for the Helen Electricity Network

The performance of different applications is discussed below in subchapters 9.1.1, 9.1.2 and 9.1.3. The research phase of the Suvilahti battery ended in summer 2019 and the battery will be connected to the aggregation platform of Helen and utilized in the TSO ancillary markets in the future.

9.1.1 Reserve power as a service for TSO

The frequency regulation has been tested with several regulation curves. The different curves are presented in Figure 41 - Figure 44. Figure 43 and Figure 44 represent the current FCR-N market rules that are to be applied for example in the commercially sold solutions.



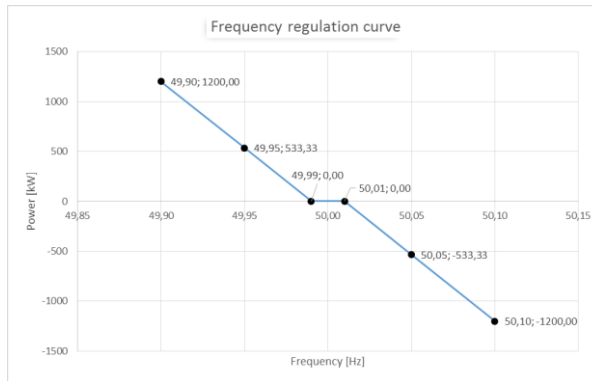


Figure 41: Target SOC was 50 % and the recovery power to target SOC during frequency dead band was 0 kW/200 kW

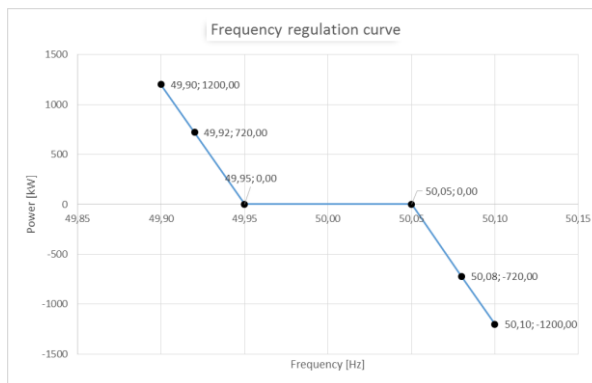


Figure 42: Target SOC was 50 % and the recovery power to target SOC during frequency dead band was 0 kW/200 kW.

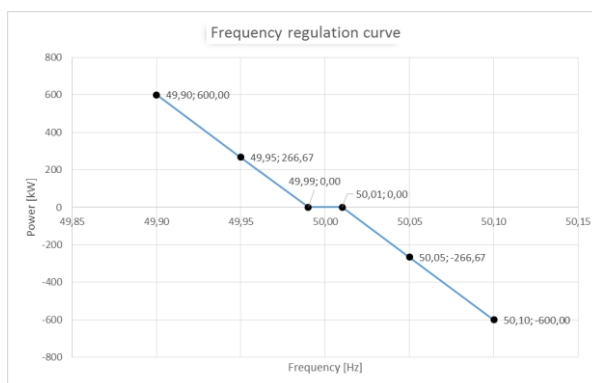


Figure 43: Target SOC was 50 % and the recovery power to target SOC during frequency dead band was 0 kW/200 kW

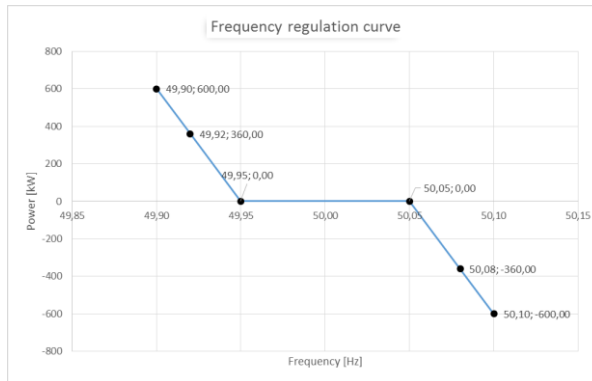


Figure 44: Target SOC was 50 % and the recovery power to target SOC during frequency dead band was 200 kW.

The main drivers with the tests have been to verify the technical capability and the limitations of the BESS and prove to the TSO that the BESS is a fast and flexible resource in restoring the grid stability. The tests have also shown that the current market for FCR-N (Frequency Containment Reserve for Normal operation) is not the best for the battery since the fast-reacting battery is competing with slower turbines and hydropower and its true value cannot be fully actualized. The tests have given proof that additional market place for fast and short regulation would be needed, also due to the decreasing inertia in the national grid.

The SOC behaviour corresponding the regulation according to the curve in Figure 41-Figure 44 is shown in Figure 45 until Figure 50.

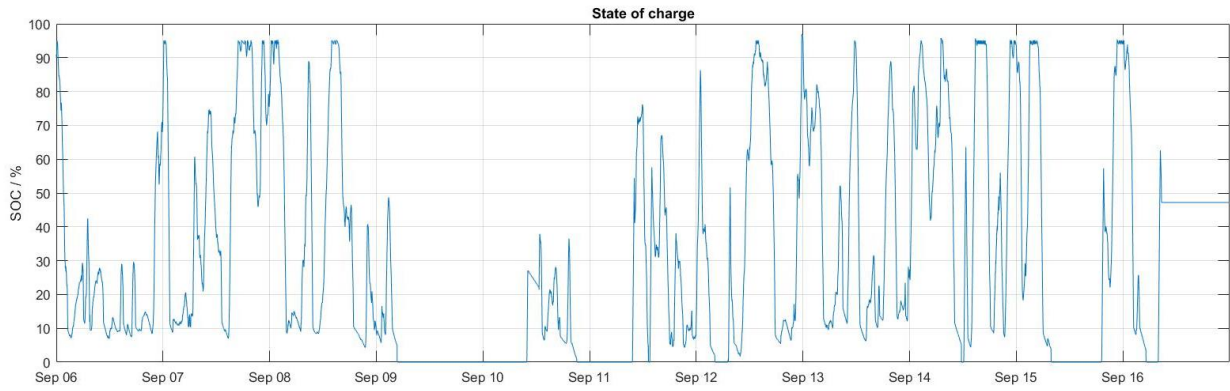


Figure 45: The SOC behaviour corresponding the regulation according to the curve in Figure 41 and recovery power to target SOC being 0 kW.

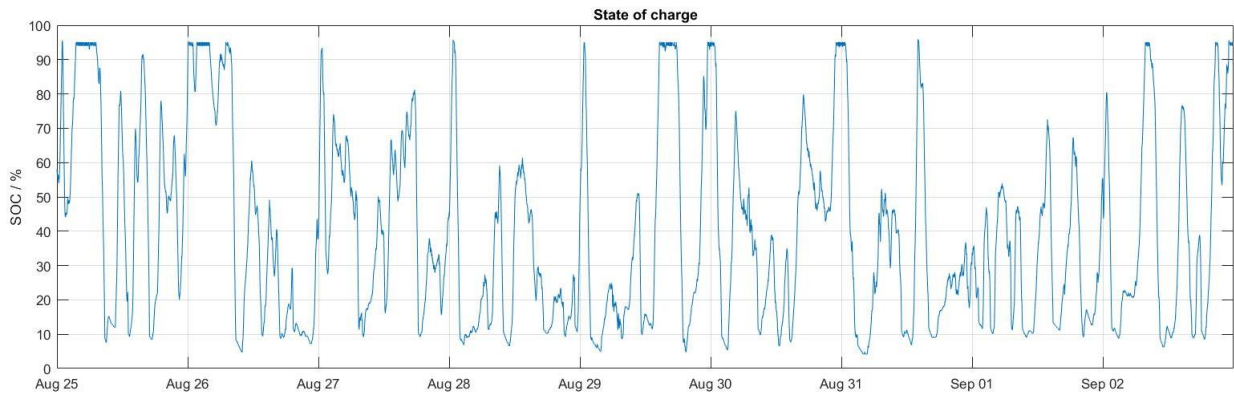


Figure 46: The SOC behaviour corresponding the regulation according to the curve in Figure 41 and recovery power to target SOC being 200 kW.

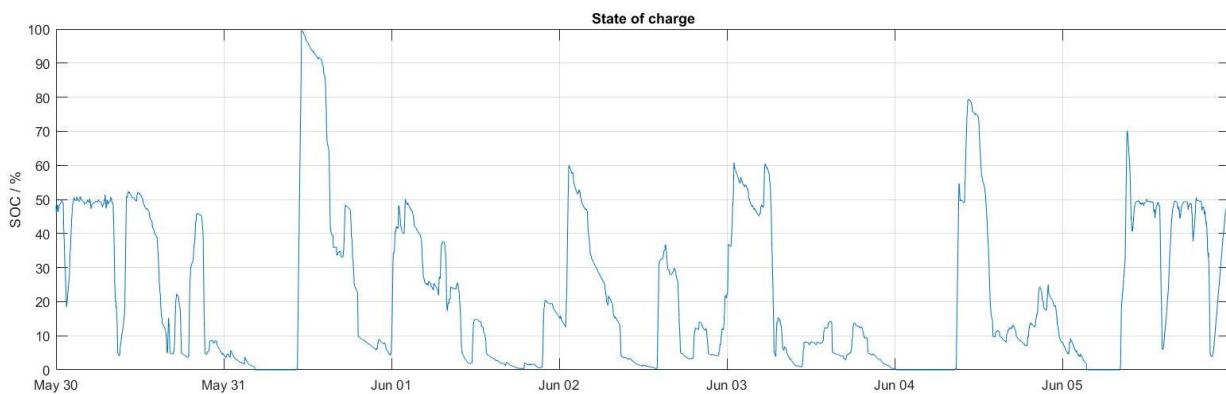


Figure 47: The SOC behaviour corresponding the regulation according to the curve in Figure 42 and recovery power to target SOC being 0 kW.

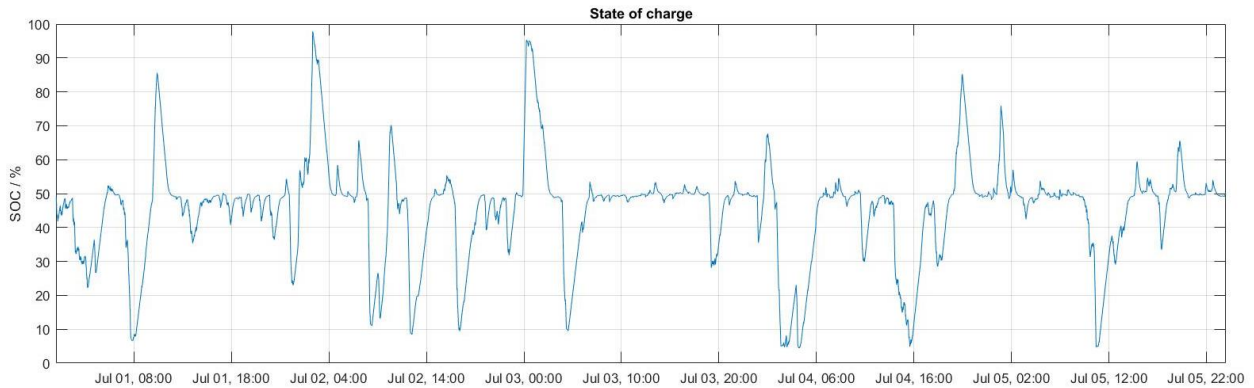


Figure 48: The SOC behaviour corresponding the regulation according to the curve in Figure 42 and recovery power to target SOC is 200 kW.

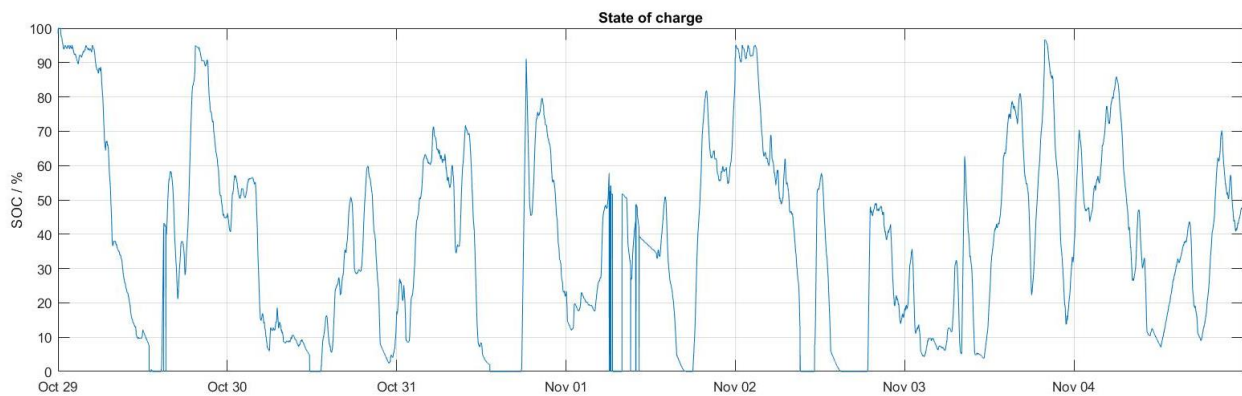


Figure 49: The SOC behaviour corresponding the regulation according to the curve in Figure 43 and recovery power to target SOC being 0 kW (until 2nd November)/200 kW.

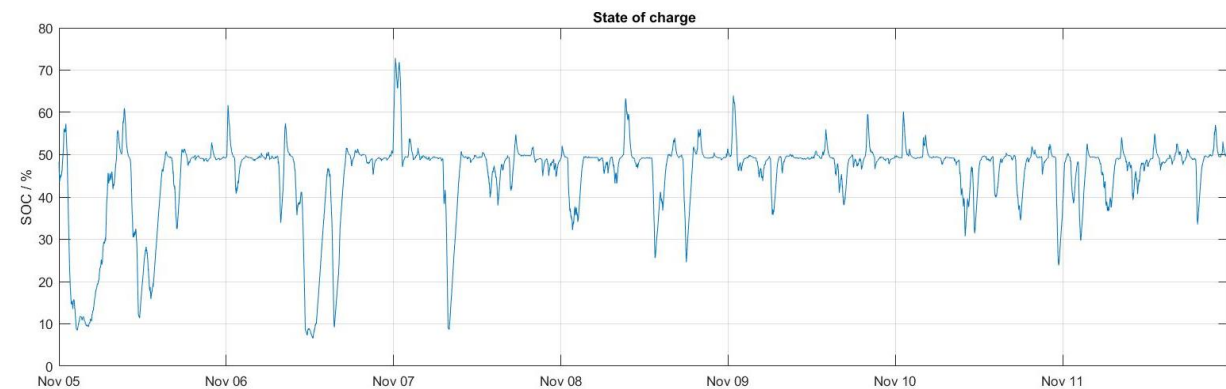


Figure 50: The SOC behaviour corresponding the regulation according to the curve in Figure 44 and recovery power to target SOC is 200 kW.

The studies have shown that the control parameters and the curve altogether have a role in how the BESS performs. The availability for service provision with different regulation curves is detailed in Table 4.

As a conclusion, the BESS performs best when the dead band is 50 mHz and a reasonable recovery power during the dead band is applied. The TSO market rules are changing in terms of dead band-width and after 2020, in FCR-N market the dead band is required to be 10 mHz. Based on the tests, Helen suggests that reasonable recovery power, such as 200 kW could be used during 10 mHz dead band to improve the availability.

In the tests, Helen has been running frequency regulation every day around the clock. In real market operation, the need for frequency regulation is determined by the market (the TSO), who accepts the bids. It is reasonable to assume that every bid is not going to be accepted which gives some recovery time for the BESS and presumably improves also the availability.

Table 4: The availability for frequency regulation with different control parameters. 1C corresponds to a system where the power ratio to the energy is equal to one, e.g. in this case 600 kW / 600 kWh and 2 C corresponds to a system where power is double to the energy, e.g. in this case 1200 kW / 600 kWh.

Duration of test period (days)	1C / 2C	Dead band width (mHz)	Recovery power (kW)	Availability (%)
7	1 C	10	0/200	83
7	1 C	50	200	100
7	2 C	10	0	66
9	2 C	10	200	92
6	2 C	50	0	81
7	2 C	50	200	99

9.1.2 Peak shaving and time-shifting

The Suvilahti BESS has been tested to smoothen e.g. metro peaks, PV production and dynamic office loads. The battery measures the input power every second and calculates a moving average. The moving average is then compared to the measured value and the BESS is charged or discharged according to the difference. In Figure 51 is shown for instance the metro load during one weekday. The same weekday is then zoomed in and shown in parallel with BESS power and combined output power in Figure 52.

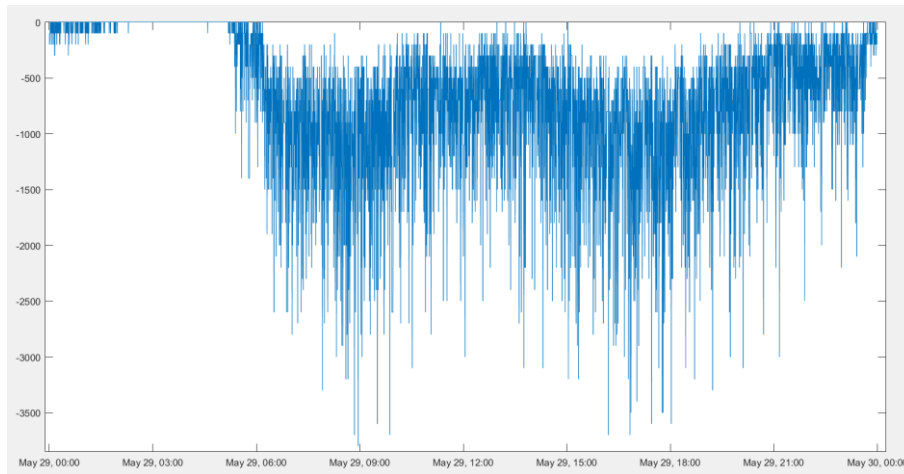


Figure 51: Metro load causes varying power needs due to the acceleration and braking at the station.

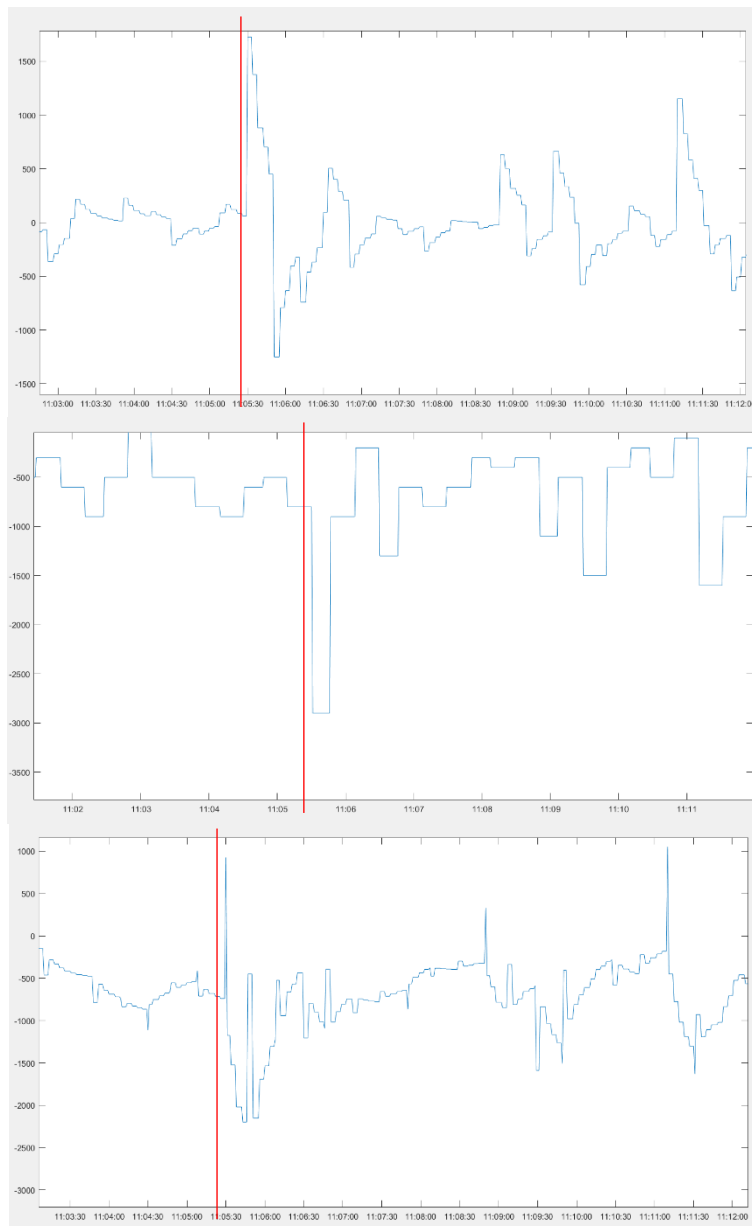


Figure 52: The battery (top) reacts to the metro peak power (middle) instantly and the reduced grid load is shown at the bottom.

9.1.3 Voltage support and reactive power compensation

The reactive power is compensated for the DSO needs. During the last years, one observed power quality concern is the considerable transition of the reactive power from the inductive to the capacitive side. The BESS is well suited to reactive power compensation since it can supply simultaneously both active and reactive power.

Suvilahti BESS assisted the DSO's reactive power management according to three modes: to balance the reactive power flow in the TSO/DSO connection point (setpoint value -900 kvar), to decrease the reactive power losses in the supplying primary 110/10 kV transformer (setpoint value 900 kvar) and, to minimize the losses of the BESS itself (setpoint value 0 kvar). In Figure 13 one week of the BESS operation in reactive power compensation is shown.

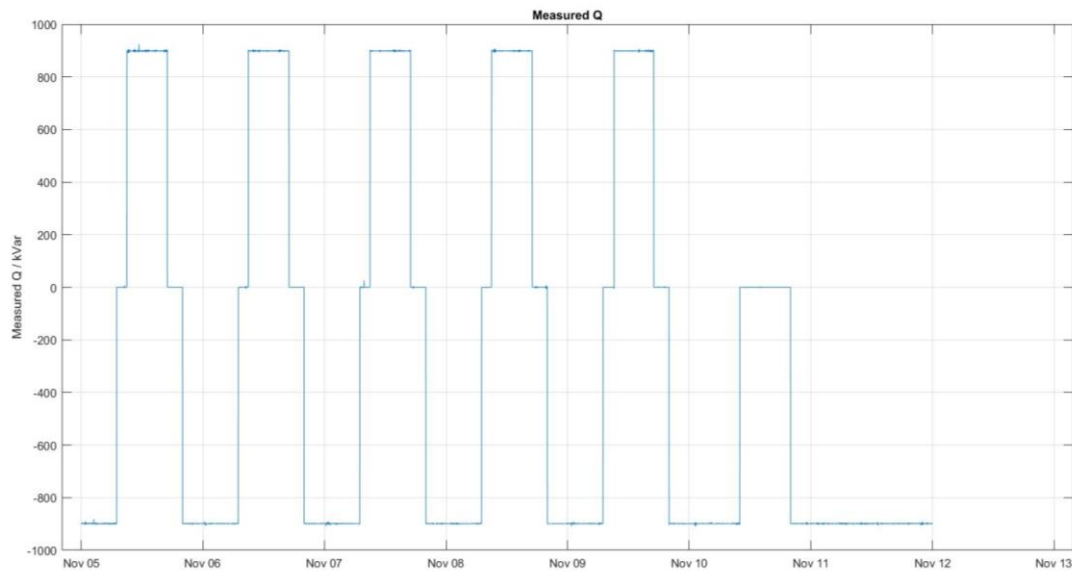


Figure 53: Reactive power compensation with the calendar-based schedule which takes into account the DSO needs.

The BESS has also been tested in voltage control, but since the DSO does not have quality issues in their grid, the operation presented in Figure 53 is more preferred. Figure 54 illustrates one week of operation where the BESS switches between reactive power compensation with -900 kvar and linear voltage control between 10,41 kV and 10,11 kV, where reactive power varies between -900 kvar and 900 kvar.

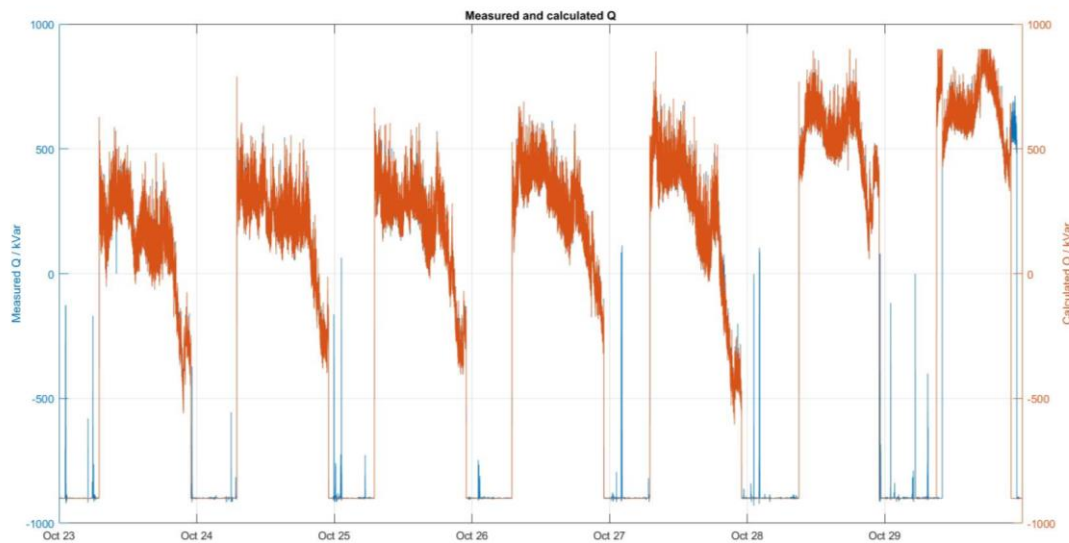


Figure 54: The BESS providing both voltage control and reactive power compensation depending on the time of the day

9.2 Performance tests with Suvilahti V2G charger

The two-way charging point was installed in Suvilahti in cooperation between Helen, Liikennevirta and Nissan in 2017. In two-way charging, vehicle battery can be used as an electricity storage unit, and it can be charged and discharged to maintain electricity network frequency. Charging and discharging capacity of the V2G charger is 10 kW and during its installation, it was the first V2G charger in Finland (Helen News 2017).

During mySMARTLife, Helen has tested the operation of V2G at the Suvilahti pilot site. Three performance tests were conducted on the V2G charger in Suvilahti in October 2018. The objective of the tests was to determine the dynamic power response capability of the charger to power regulation commands sent from the Virta Energy mobile user interface. During mySMARTLife project, the V2G charger was connected to Virta back-end as well as to Virta Energy UI. Virta Energy UI was used during the tests to manually control the charger power requests. The connected test vehicle was Nissan eNV200 supplied by Helen. A wireless clamp current meter was used to measure the DC current flowing between the charger and the connected vehicle. A manual stopwatch was used to determine the time between giving power command via the Virta Energy mobile UI and the response shown by the clamp current meter. The test runs were conducted so that the power commands were given from the Virta Energy UI every 10 seconds, as measured with a constantly running timer on a manual stopwatch.

9.2.1 Test 1 - Up and down regulation in 5 kW steps at 10 seconds intervals

The results of the first test run are shown in Figure 55. The blue areas in the figure show the requested charger power as commanded by the Virta Energy UI and the orange line shows the DC power response of the charger as calculated from the current measured with the meter.

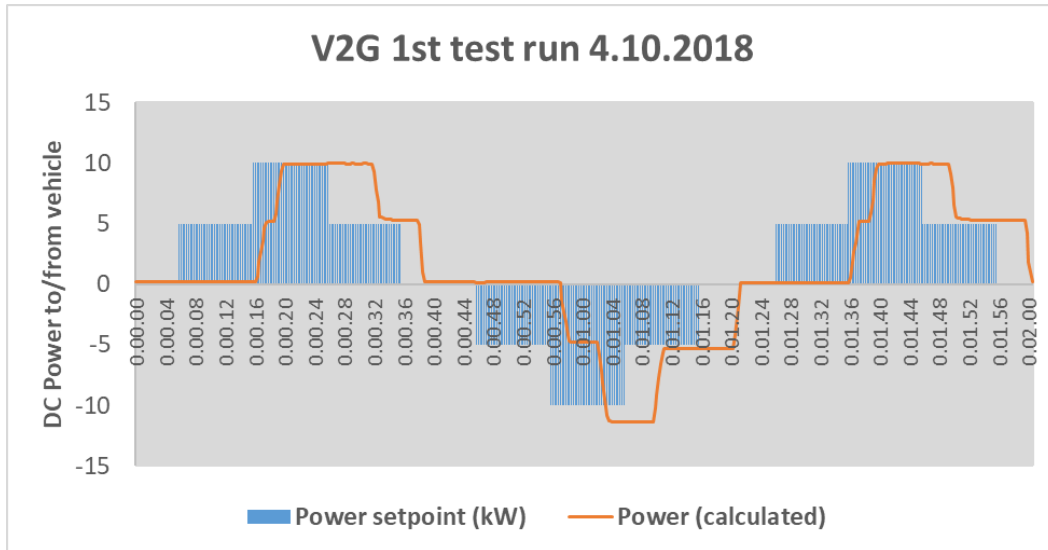


Figure 55: The requested power profile and actual response of the charger during the test 1.

The measurement results show two key findings:

- The delay between giving a power request from the Virta Energy UI and actual power response from the charger is between 4-10 seconds.
- The delay is not uniform but appears to vary depending on the direction of the power request compared to the previous state of the charger.

9.2.2 Test 2 – Up & down power regulation in 1 kW steps at 10 second intervals

The results of the second test run are shown in Figure 56. The blue areas in the figure show the requested charger power as commanded by the Virta Energy UI and the orange line shows the DC power response of the charger as calculated from the current measured with the current meter.

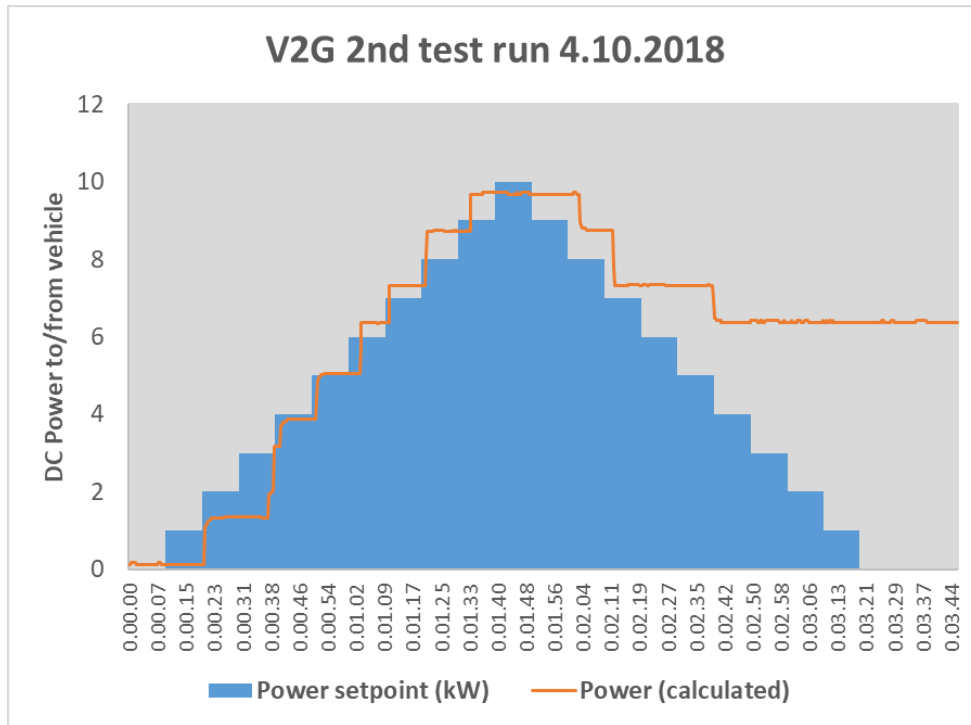


Figure 56: The requested power profile and actual response of the charger during test 2.

The measurement results show several key findings:

- The delay between giving a power request from the Virta Energy UI and actual power response from the charger is between 4-10 seconds.
- The delay is not uniform and the power response as compared to the request is not consistent
- Some power steps given in Virta Energy UI appear to have been missed by the charger (note: there are 10 power steps of 1 kW given in the Virta Energy UI but the charger reached the maximum requested output in fewer steps).
- The charger became unresponsive after 2 minutes and 10 seconds in the test. The charger had to be physically restarted (hard reset) to become responsive again.

9.2.3 Test 3 - composite run with different power regulation steps at 10 second intervals

The results of the final test run are shown in Figure 57. The blue areas in the figure show the requested charger power as commanded by the Virta Energy UI and the orange line shows the DC power response of the charger as calculated from the current measured with current meter.

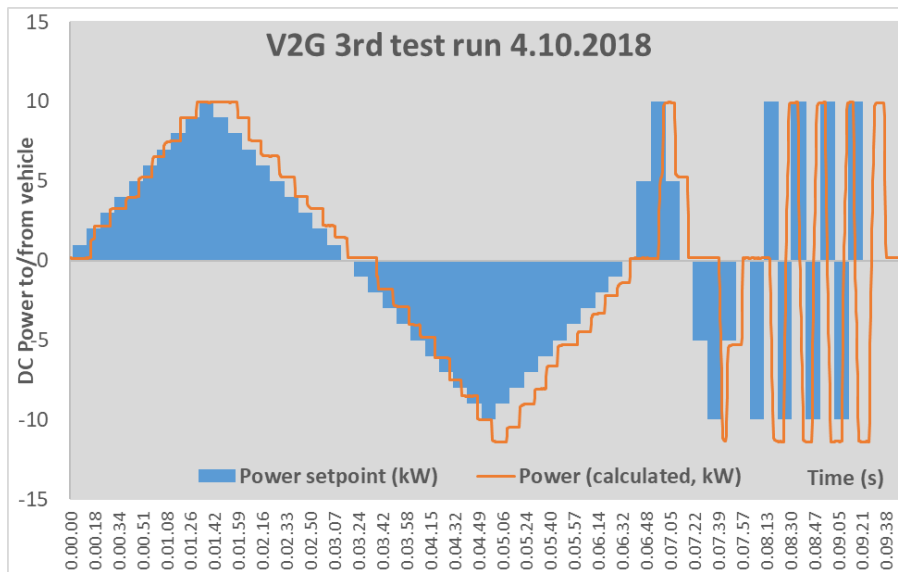


Figure 57: The requested power profile and actual response of the charger during test 3.

The measurement results show several key findings:

- The delay between giving a power request from the Virta Energy UI and actual power response from the charger is between 4-10 seconds.
- The delay is not uniform and the power response as compared to the request is not consistent
- Some power steps given in Virta Energy UI appear to have been missed by the charger
- The charger appears to discharge the EV battery with a higher power level than charge
 - Power set point of +9 kW and +10 kW in the Virta Energy UI resulted in the same charging power of 10 kW as calculated from the current measured by the meter.
 - Power set point of -10 kW in the Virta Energy UI resulted in discharging power of -11 kW as calculated from the current measured by the meter.

9.2.4 Assumptions and possible sources or errors during the tests

Possible sources of errors and assumptions in the above mentioned three tests may include:

- Only the DC current flowing between the vehicle and charger was measured. The charging / discharging power was calculated from the DC current using a fixed 440 V DC charge voltage estimate.
 - The changes in charging/discharging voltage of the EV battery pack that occur due to changes in internal resistance during the test are not accounted for. The internal

resistance and voltage are affected by the charging/discharging power level and battery state of charge (SOC).

- The effect of battery SOC is considered negligible, as the short test runs did not markedly change the battery SOC. However, the change of EV battery internal resistance and voltage due to different power levels introduce some systematic error in the calculated power values.
- The test runs were conducted so that the power commands were given from the Virta Energy UI every 10 seconds, as measured with a constantly running timer on a manual stopwatch. The human margin of error in issuing the commands in time via the Virta Energy UI is estimated to be +/- 1 second.

9.2.5 Summary and conclusions of the tests with Suvilahti V2G

The objective of the tests was to determine the dynamic power response capability of the charger to power regulation commands sent from the Virta Energy mobile user interface. The charger was able to regulate the charging and discharging power according to commands issued from the Virta Energy UI within a 4-10 second response time. The delay in response appears to be slightly related to the direction of the power request to the charger. The accuracy of the actual power regulation compared to power command could not be verified due to only having DC current measured and logged during the tests.

The speed of actual power output change, not including the response delay caused by back end communication, shows promise for grid frequency control applications. However, the 4-10 second total system response time is not acceptable in the fastest TSO ancillary markets and therefore the response time should be shortened in future applications if ancillary market usage is considered. The technology of V2G chargers has improved already in a few years period and it is expected that the V2G chargers will be a part of future systems.

10. Conclusions

This deliverable studied the integration of EV charging and battery storage on the power system infrastructure and operation. It reviewed literature and demonstrations on smart charging, analyzed EV charging data from Helsinki, and developed control strategies for the co-operation of BESS, PV, and EV charging. Currently, the emergence of EV aggregator seems to be a viable approach to implement the power system integration of EV charging. The aggregators supply electricity to their customer EVs, while they can also exploit the charging load and EV batteries to provide ancillary services and flexibility to the

power system. On the other hand, EVs are a form of distributed resource, which can actively participate in the matching of local generation and consumption.

The investigated control strategies for the co-operation of BESS, PV, and EV charging can be used to reduce the energy exchange with the grid, that is, to improve the self-sufficiency of a consumer. However, the battery easily becomes empty or full if the control parameters are not properly selected. The system performance is greatly affected by the control logic the BESS employs when providing frequency regulation. For future studies, the performance might be possible to improve with predictive approaches. They would take into account coming PV generation and charging and adjust the control accordingly. However, the BESS operation is mainly dictated by the frequency control, of which energy and power requirements are difficult to predict.

The deliverable also analyzed the EV charging data of public charging stations from Helsinki. Generally, the analysis revealed that there is some flexibility available in the charging load at least for short charging interruptions. The challenge is the low charging load due to a small number of charging events per day. Few EVs are charging and the charging typically lasts only a short time. Nevertheless, the data provide promising input for simulations of larger EV fleet and their flexibility for future studies.

Furthermore, this report provides information about the different field tests done with the Suvilahti Battery as well as a V2G charger in Suvilahti pilot site. The research phase finished in summer 2019 and now the battery is targeted to operate in TSO ancillary markets.

All in all, this research demonstrate the potential of EV charging station and large battery storage system on providing ancillary services for power grids having large share of renewable energy sources and studied business case for practical implementation.

11. References

- Alahäivälä, A., 2012. Electric vehicle charging and its impact on distribution transformers in urban area, Master's Thesis, Aalto University.
- Alahäivälä, A. and Lehtonen, M., 2015, November. Coordination strategies for distributed resources as frequency containment reserves. In *Innovative Smart Grid Technologies-Asia (ISGT ASIA), 2015 IEEE* (pp. 1-6).
- Bhatti, A.R., Salam, Z., Aziz, M.J.B.A. and Yee, K.P., 2016. A critical review of electric vehicle charging using solar photovoltaic. *International Journal of Energy Research*, 40(4), pp.439-461.
- BMW i ChargeForward, 2017. PG&E's Electric Vehicle Smart Charging Pilot. Project report. Available at: <http://www.pgecurrents.com/wp-content/uploads/2017/06/PGE-BMW-iChargeForward-Final-Report.pdf>
- Eurelectric, 2015. Smart Charging: steering the charge, driving the change. Project report. Available at: http://www.eurelectric.org/media/169888/20032015_paper_on_smart_charging_of_electric_vehicles_final_psf-2015-2301-0001-01-e.pdf
- E. Julia Merino , Inés Gómez , Elena Turienzo, " *SmartNet Project D1.1: Ancillary service provision by RES and DSM connected at distribution level in the future power system,*" 2016.
- Fingrid, 2018. Reserve Market Information. Available at: https://www.fingrid.fi/en/electricity-market/reserves_and_balancing/reserve-market-information/
- García-Villalobos, J., Zamora, I., San Martín, J.I., Asensio, F.J. and Aperribay, V., 2014. Plug-in electric vehicles in electric distribution networks: A review of smart charging approaches. *Renewable and Sustainable Energy Reviews*, 38, pp.717-731.
- Ghazvini, M.A.F., Faria, P., Ramos, S., Morais, H. and Vale, Z., 2015. Incentive-based demand response programs designed by asset-light retail electricity providers for the day-ahead market. *Energy*, 82, pp.786-799.
- Hasanpor Divshali. P, Evens, E., „Behaviour Analysis of Electrical Vehicle Flexibility Based on Large-Scale Charging Data“, IEEE conference on PowerTec, Milan, 2019
- Helen News 2017. <https://www.helen.fi/uutiset/2017/v2g>
- Hellman, H.P. et al., 2017, June. Benefits of battery energy storage system for system, market, & distribution network - case Helsinki. In *24th International Conference on Electricity Distribution (CIRED)*.
- Hu, J., Morais, H., Sousa, T. and Lind, M., 2016. Electric vehicle fleet management in smart grids: A review of services, optimization and control aspects. *Renewable and Sustainable Energy Reviews*, 56, pp.1207-1226.

- IZEUS, 2014. Smart Grid and Smart Traffic Services for Electric Mobility. Webpage. Available at: <http://www.izeus.kit.edu/english/62.php>
- Kisacikoglu M., 2016. EV-Grid Integration (EVGI) Control and System Implementation—Research Overview. Presentation. Available at: <https://www.nrel.gov/docs/fy16osti/65861.pdf>
- Madina, C., Zamora, I. and Zabala, E., 2016. Methodology for assessing electric vehicle charging infrastructure business models. *Energy Policy*, 89, pp.284-293.
- Mégel, O., Mathieu, J.L. and Andersson, G., 2013, October. Maximizing the potential of energy storage to provide fast frequency control. In *Innovative Smart Grid Technologies Europe (ISGT EUROPE), 2013 4th IEEE/PES* (pp. 1-5).
- Nolan Ritter, Sarah Darby, Juha Forsström, Sarah Higginson, Göran Koreneff, Lassi Similä, Wolf-Peter Schill, Stefanie Reiss, Marina Topouzi, Alexander Zerrahn, 'H2020 REALVALUE Deliverable D6.3: Market Design and Business Models Report', 2016
- Nunes, P., Figueiredo, R. and Brito, M.C., 2016. The use of parking lots to solar-charge electric vehicles. *Renewable and Sustainable Energy Reviews*, 66, pp.679-693.
- Pudjianto, D., Ramsay, C. and Strbac, G., 2007. Virtual power plant and system integration of distributed energy resources. *IET Renewable Power Generation*, 1(1), pp.10-16.
- San Román, T.G., Momber, I., Abbad, M.R. and Miralles, A.S., 2011. Regulatory framework and business models for charging plug-in electric vehicles: Infrastructure, agents, and commercial relationships. *Energy policy*, 39(10), pp.6360-6375.
- SEEV4-City, 2017. Operational Pilots. Webpage. Available at: <http://www.northsearegion.eu/seev4-city/operational-pilots/>
- Smart Solar Charging, 2017. Presentation. Available at: <https://husite.nl/ssc2017/wp-content/uploads/sites/146/2017/06/9-P3-Smart-solar-charging-van-Sark.pdf>
- Stevens M., 2016. ChargeTO Smart-Charging Pilot. Presentation. Available at: <https://evroadmapconference.com/program/presentations16/MattStevens.pdf>
- Wi, Y.M., Lee, J.U. and Joo, S.K., 2013. Electric vehicle charging method for smart homes/buildings with a photovoltaic system. *IEEE Transactions on Consumer Electronics*, 59(2), pp.323-328.

